Title	Review of pH sensing materials from macro- to nano-scale: Recent developments and examples of seawater applications
Authors	Avolio, Roberto;Grozdanov, Anita;Avella, Maurizio;Barton, John;Cocca, Mariacristina;De Falco, Francesca;Dimitrov, Aleksandar T.;Errico, Maria Emanuela;Fanjul-Bolado, Pablo;Gentile, Gennaro;Paunovic, Perica;Ribotti, Alberto;Magni, Paolo
Publication date	2020-11-16
Original Citation	Avolio, R., Grozdanov, A., Avella, M., Barton, J., Cocca, M., De Falco, F., Dimitrov, A. T., Errico, M. E., Fanjul-Bolado, P., Gentile, G., Paunovic, P., Ribotti, A. and Magni, P. (2020) 'Review of pH sensing materials from macro- to nano-scale: Recent developments and examples of seawater applications', Critical Reviews in Environmental Science and Technology, 52(6), pp. 979-1021. doi: 10.1080/10643389.2020.1843312
Type of publication	Article (peer-reviewed)
Link to publisher's version	10.1080/10643389.2020.1843312
Rights	© 2020, Taylor & Francis Group, LLC. This is an Accepted Manuscript of an item published by Taylor & Francis in Critical Reviews in Environmental Science and Technology on16 November 2020, available online: https://doi.org/10.1080/10643389.2020.1843312
Download date	2025-08-03 06:17:40
Item downloaded from	https://hdl.handle.net/10468/13230

University College Cork, Ireland

Coláiste na hOllscoile Corcaigh

University College Cork, Ireland

Coláiste na hOllscoile Corcaigh

1 **Review of pH sensing materials from macro- to nano-scale: recent**

2 **developments and examples of seawater applications**

3

4 Roberto Avolio*[a], Anita Grozdanov[b], Maurizio Avella[a], John Barton[c], Mariacristina Cocca[a],

5 Francesca De Falco[a], Aleksandar T. Dimitrov[b], Maria Emanuela Errico[a], Pablo Fanjul-

6 Bolado[d], Gennaro Gentile[a], Perica Paunovic[b], Alberto Ribotti[e], Paolo Magni*[e,f]

7

8

9 [a] National Research Council of Italy, Institute for Polymers Composites and Biomaterials (CNR-IPCB),

10 Via Campi Flegrei 34, 80078 Pozzuoli (NA), Italy

11 [b] Faculty of Technology and Metallurgy, Ss. Cyril and Methodius University in Skopje, Skopje, North

12 Macedonia

13 [c] Tyndall National Institute, University College Cork, Lee Maltings Complex, Dyke Parade, Cork,

14 T12R5CP, Ireland

15 [d] Metrohm DropSens, Vivarium Ciencias de la Salud, C/Colegio Santo Domingo de Guzmán, 33010,

16 Oviedo, Spain

17 [e] National Research Council of Italy, Institute for the Study of Anthropogenic Impact and Sustainability

18 in Marine Environment (CNR-IAS), 09170 Oristano, Italy

19 [f] Foundation International Marine Centre (IMC), Loc. Sa Mardini, Torregrande, 09170, Oristano, Italy

20

21 *Corresponding authors: roberto.avolio@ipcb.cnr.it; paolo.magni@cnr.it

22

23

24 ORCID:

25 Roberto Avolio: https://orcid.org/0000-0002-5733-0161

26 John Barton https://orcid.org/0000-0002-0671-5678

27 Pablo Fanjul-Bolado: https://orcid.org/0000-0002-9224-1666

28 Alberto Ribotti: https://orcid.org/0000-0002-6709-1600

29 Paolo Magni: https://orcid.org/0000-0001-5955-6829

Abstract

Over the last decades, a large number of pH sensitive materials with new compositions and structures have been proposed. Solid state sensors based on organic, inorganic and composite materials are actively investigated, with an increasing interest in the performances offered by nano-scale materials. Our review provides a thorough, up-to-date knowledge of a wide range of pH measurement methods and related-sensing materials, first introducing well established materials and methods for pH sensing and then covering recent developments in inorganic, organic and nano-engineered devices. The main sensor parameters, including sensitivity, stability, response time and testing conditions are reported. Given the importance of pH sensing in environmental applications, in particular seawater monitoring, sensors tested in seawater are highlighted and discussed.

Key words: pH sensors; environmental monitoring; nanomaterials; water quality

1. Introduction

Due to the relevance of pH for many chemical and biochemical processes, pH measurements are routinely carried out in a very broad range of activities, from industrial processes to chemistry, medicine and environmental monitoring.

pH strongly affects environmental and biological processes. The availability of nutrients, the uptake of pollutants like heavy metals, the occurrence and distribution of microorganisms, the efficiency of enzymatic bioprocesses and metabolism, the occurrence of oxidative stress and its consequences on living organisms, are all pH-related phenomena (González Durán et al., 2018; Jin & Kirk, 2018; Kahn et al., 2017). Accurate quantification of pH is then vital for monitoring and protecting the health of our planet. In particular, pH is intimately linked with the dynamics of nutrients, contaminants, and trace metals in seawater and is entangled with the complex ocean carbonate system. As the pH of ocean surface decreases (-0.15 since pre-industrial times due to increasing dissolution of atmospheric CO_2, Clarke et al., 2015), the delicate equilibria among chemical species in solution are perturbed, with effects on coastal biodiversity, ecosystem functioning (Lacoue-Labarthe et al., 2016) and the health of ecosystems worldwide (Kroeker et al., 2013; Somero et al., 2016). Continuous, accurate and punctual recording of seawater pH is needed to increase our understanding of the local and global pH dynamics and enable a better prediction of their effects (Bushinsky et al., 2019; Stow et al., 2009).

Ion sensitive glass electrodes are the most popular pH sensors, due to their reliability, affordability and fast (few s) response time. This includes environmental applications like seawater monitoring and most oceanic probes are equipped with this kind of pH sensors for routine pH recording. However, glass electrodes exhibit signal instability or drift and, therefore, require constant re-calibration: this operation can cause significant error, that may arise from the quality and handling of the calibration solutions (McLaughlin et al., 2017b). The need for an inner electrolyte solution, connecting the reference electrode with the sample solution through a liquid junction, can be another source of error as the potential that develops across the junction varies as a consequence of external factors like pressure. Finally, glass electrodes are brittle, need a storage solution and cannot be miniaturized.

For all these reasons, a number of alternative pH sensing devices have been proposed over the past decades. High precision measurements (up to 0.001 pH units) can be provided by spectrophotometric devices that are, however, much more expensive and complex than potentiometric sensors and have long sampling time (up to minutes). Solid state sensors can provide a cheap, robust and miniaturizable alternative for pH measurements (Korostynska et al., 2007), as demonstrated by the presence on the market of Ion Sensitive Field-Effect Transistors (ISFETs) based pH probes. These features can be exploited to realize sensing system with low cost, low power consumption and ease of operation (Radu et al., 2015). In the case of seawater monitoring, desired uncertainties for pH sensing have been specified as 0.02 for the study of short term, local variation and 0.003 for global, long term trends (Newton et al., 2015) and the quest for sensors with optimal field performances is

80   still open (Okazaki et al., 2017). A discussion of problems and techniques related to the measurement

81   of pH in marine waters can be found in specialized papers (Byrne, 2014; Marion et al., 2011).

82   This review will discuss developments in the field of solid-state pH sensors, covering organic,

83   inorganic and composite sensing materials and focusing on recent devices based on nanomaterials.

84   Parameters like sensitivity, stability, robustness to interfering ions and response time of the sensors

85   will be reported and organized in tables for a fast reference. Recent examples of pH sensors

86   developed for seawater applications will be provided and critically reviewed at the end of each

87   chapter. Providing a thorough, up-to-date knowledge of a wide range of pH measurement methods

88   and related-sensing materials, our review may assist materials scientists, sensors developers and

89   marine scientists interested in new pH sensing solutions.

90

2. Traditional methods and materials for pH measurement

92   The hydrogen ion is a ubiquitous species that plays a role in most chemical and biochemical reactions

93   carried out in aqueous solutions. Firstly introduced by the Danish biochemist Soren Peter Lauritz

94   Sorensen, pH is defined as the negative logarithm of H$^+$ activity (Sørensen, 1909; Buck et al., 2002):

95   $$pH = -\log(a_{H^+}) \qquad (1)$$

96   Due to the importance of this parameter for a wide range of applications, pH measurements are

97   routinely performed in chemical, industrial, biological and medical practice. In the following sections,

98   well established measurement techniques will be summarized, introducing some examples of

99   seawater-designed devices.

100   **2.1 Optical/spectrophotometric methods**

101   A practical measurement of pH can be obtained using the so-called acid-base indicators, substances

102   that change their color as a function of pH. In general, an indicator dye is an amphoteric compound

103   with a dissociation constant that is close to the pH to be determined. The pH of the sample-indicator

104   system can be expressed as a function of the dissociation constant of the indicator (pK) and of the

105   concentration of its protonated (HA) and unprotonated (A$^-$) form:

106   $$pH = pK + \log\frac{[A^-]}{[HA]} \qquad (2)$$

107   As the two forms of the indicator in solution have different colors due to different light absorption, their

108   concentration can be measured from their absorption spectra.

109   Based on this principle, spectrophotometric methods for pH measurement, reaching an accuracy as

110   high as 0.001, have been developed using different indicators such as m-cresol purple, cresol red,

111   bromocresol green, bromocresol purple and thymol blue (King & Kester, 1989; Millero et al., 2009). A

112   schematic example of automated spectrophotometric pH system is reported in Figure 1. Once

113   calibrated, these devices do not need to be recalibrated for use at sea. A description of a

114   spectrophotometric pH sensor designed for in situ measurements can be found in Cullison Gray et al.

115   (2011) and in Lai et al. (2018).

116 Recent technological developments of optical/spectrophotometric-based sensors represent a
117 promising tool for monitoring the ocean carbonate system. In particular, pH sensors using
118 spectrophotometric techniques are currently used for surface water measurements on research
119 vessels and, similarly, optodes for pCO_2 measurements have been successfully tested in seawater for
120 oceanographic applications (Rérolle et al., 2018; Staudinger et al., 2018; 2019 and references
121 therein). Optical methods for pH detection will not be further discussed. A comprehensive review can
122 be found in (Rérolle et al., 2012).

123 **2.2 Electrochemical methods**

124 Probably the most common techniques for pH sensing are based on the measurement of electrical
125 parameters, such as conductivity or resistivity, impedance, potential. Conductometric devices
126 correlate the change in conductivity/resistivity of an active material connecting two electrodes to the
127 concentration of the analyte (H^+ for pH). Voltammetric devices measure the current flowing between
128 the electrodes when the potential is swept in a defined manner; in this case, the pH measurement can
129 be correlated to a peak potential of an electroactive compound (Dai et al., 2016).

130 Potentiometric sensors are the most used for routine pH determination. In principle, a potentiometric
131 measurement consists of the measurement of the electromotive force (EMF) in an electrochemical
132 cell, composed of a working electrode and a reference electrode. The pH of the sample is calculated
133 comparing the EMF measured in the sample (E_s) and in a standard buffer solution (E_b) of known pH
134 (pH_b), following the Nernst equation:

135 $$pH = pH_b + \frac{(E_b - E_s)F}{RTln10} \qquad (3)$$

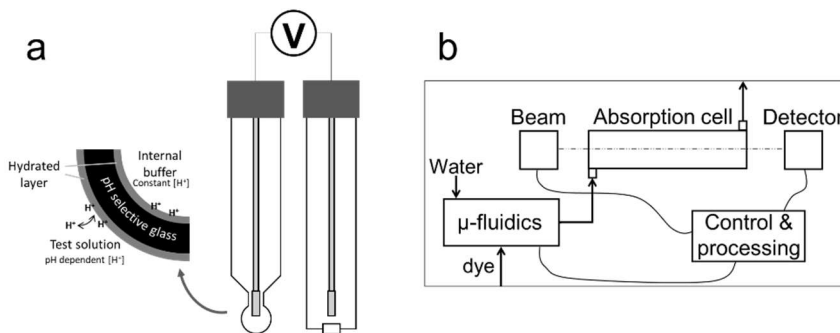136 where R is the gas constant, F is the Faraday constant and T is the temperature (Rérolle et al., 2012).

138 **Figure 1.** Scheme of: a potentiometric pH sensor with glass ion sensitive electrode (a) and a spectrophotometric
139 pH measurement device (b).

140 The most used working electrode for this application is made of a silver/silver chloride electrode
141 embedded into a glass tube that ends in an ion selective glass membrane. On both sides of the glass
142 membrane, a hydrated gel layer is formed with the aqueous solutions that are in contact with glass
143 surfaces (Figure 1). The concentration of H^+ ions on the inner layer, containing a reference solution, is
144 constant while on the outer layer it varies depending on pH. As a consequence, there is an exchange
145 of alkaline ions between the outer layer and the glass membrane that changes the overall potential of

146 the membrane. The reference electrode is usually of the same type (Ag/AgCl), immersed into a KCl

147 solution and can be included with the working electrode in a single device.

148 The glass electrode potentiometric equipment is relatively cheap and has been the only practical way

149 to measure pH of seawater for many years. However, the glass electrodes must be handled with care

150 due to the brittleness that is associated with glass, and properly stored in electrolyte solutions to

151 prevent ions leaching from the glass membrane (if stored in deionized water) and to preserve the

152 hydrated layer onto glass surface from drying out. They also have a limited shelf life due to the

153 degradation of the glass membrane and need a regular calibration in seawater buffers, whose

154 accurate preparation determines the accuracy of the measurement (McLaughlin et al., 2017b;

155 Weldborg et al., 2009). The stability and pressure sensitivity of the "liquid junction", the porous

156 membrane that allows an ion flow to close the electrochemical cell, can also be an issue. In practice,

157 electrode potential drift and experimental problems can limit the accuracy of potentiometric

158 measurements to less than 0.01, with a drift of 0.02 pH/day (Rérolle et al., 2012).

3. Inorganic materials for solid state sensors

160 The realization of a miniaturizable, stable and cheap pH sensor to substitute glass membrane based

161 devices is still a challenge. A number of solid-state sensors have been proposed and some of them

162 are already available on the market.

163 A common approach to solid state Nernstian pH sensors is based on the realization of Ion Sensitive

164 Field Effect Transistors (ISFETs). ISFETs are traditional Metal Oxide Semiconductor Field Effect

165 Transistors (MOSFET), where the gate electrode is modified (or substituted) by a thin layer of an

166 insulating material (Si_3N_4, Al_2O_3, Y_2O_3, ZrO_2). The protonation/deprotonation process occuring on the

167 insulator layer when in contact with water solutions of different pH determines the electrostatic field at

168 the gate, controlling the current flowing into the FET (Bergveld, 2003). The circuit must be closed

169 using a reference electrode connected to the source in lieu of the now removed gate (liquid gating).

170 ISFET pH sensors exploit a mature (more than 20 years) technology and have been used extensively

171 for industrial, clinical and environmental pH monitoring as they offer a number of advantages, relative

172 to glass electrodes. First, the sensor can be fabricated with conventional silicon based semiconductor

173 technologies at reduced costs and ease of integration with electronic devices. Furthermore, it is small,

174 resistant to mechanical shock and does not need a storage solution. Due to the different structure, the

175 impedance of ISFET devices is lower with respect to glass electrodes, which has a beneficial effect

176 on noise and stability. Commercially available sensors based on ISFET technology have been tested

177 at sea with encouraging results and devices specifically designed for oceanographic research, mainly

178 based on the Honeywell Durafet™ sensor, are currently used by research institutions (Johnson et al.,

179 2016; Saba et al., 2019).

180 Despite the good performances of ISFET sensors, further refinements are required for their extended

181 use in ocean acidification studies, concerning, as an example, the reliability of the reference

182 electrode, long signal stabilization time and the stability of the sensor during long-term oceanic

183 deployments (Martz et al., 2015; McLaughlin et al., 2017a; Rérolle et al., 2012).

184   A wide number of variations to the standard ISFET design have been proposed over the years. Some
185   examples of the most advanced solutions will be reported here (see Table 1 for main parameters). A
186   double gate architecture that can push sensitivity above the Nernst limit has been developed. As an
187   example, a double gate ISFET based on ZnO was claimed, with a sensitivity as high as 2.25 V/pH
188   (Spijkman et al., 2011a). The high sensitivity is generated by a capacitive coupling effect (Spijkman et
189   al., 2011b) that, in this case, was maximized by applying an extremely thin passivation layer, a self
190   assembled monolayer of octadecyl phosphonic acid. However, the device was tested only at the pH
191   values of 6 and 8, and showed a large standard deviation in the measured potential. An alternative
192   design to reduce noise and increase stability relies on the realization of an extended sensing layer,
193   connected to the gate (extended-gate FET or EGFET; Pullano et al., 2018). Parizi et al. (2012)
194   proposed a device that couples two EGFETs (n- and p- type) in parallel, matched to have the same
195   transconductance to cancel a large part of the noise. This design allows the substitution of the
196   external reference electrode (e.g. Ag/AgCl) with a simple, solid state pseudo-reference.

197   In a recent paper, Takechi et al. (2015) demonstrated a signal amplification effect similar to Spijkman
198   (2011a) using an amorphous $InGaZnO_4$ (IGZO) layer as the bottom gate and a thin film of TaO_x as an
199   ion sensitive top gate. The resulting sensitivity is as high as 450 mV/pH but the resolution limit,
200   calculated taking into account drift and hysteresis of the device, was estimated in 0.02 pH in a narrow
201   range (pH 4 – 6). An optimization of the fabrication process led to a similar $IGZO/Ta_2O_5$ based ISFET
202   with a sensitivity of 402 mV/pH in the 4 – 9 pH range (Kumar et al., 2017). However, stability and drift
203   problems still constitute a serious limit to the use of this kind of device in demanding applications (Pyo
204   & Cho, 2017). Ta_2O_5 has been investigated also for the realization of flexible extended gate
205   electrodes, printed on plastics and coupled to a FET device (Wu et al., 2017). The sensitivity of this
206   assembly was relatively low, 24 mV/pH, but good temporal stability (drift < 1% during tests) and
207   repeatability were observed.

208   Recently, an interesting combination of organic semiconductor and SiO_x thin layer was tested as gate
209   in a dual-gate ISFET device, showing an improvement in response time and an amplification of the
210   signal up to 10 times with respect to a bare SiO_x layer (Pfattner et al., 2019). However, the stability of
211   the response was not addressed.

212   In summary, ISFET devices take advantage of well-established semiconductor fabrication processes
213   for the production and integration of pH sensors. It is a technology with a long history and a high
214   maturity level, with at least one product dedicated to seawater application already on the market. In
215   the quest for increased stability and accuracy, a number of improved designs have been proposed
216   and tested at laboratory scale. Latest developments make use of nano-engineered active layers and
217   electrodes and will be discussed in Section 5.
218

Sensing material and setup	Testing range and media	Sensitivity	Stability	Response time	Reference
ZnO Dual gate ISFET	6 – 8 Commercial buffers	Up to 2.25 V/pH	Low hysteresis.	n/a	Spijkman et al., 2011a

			High standard deviation on sensitivity estimation.		
Al$_2$O$_3$ EGFET	4 – 10	Up to 130 mV/pH	n/a	n/a	Parizi et al., 2012
TaO$_x$ Dual gate ISFET	4 – 6 McIlvaine buffer (Na$_2$HPO$_4$ – citric acid)	453 mV/pH Resolution up to 0.02 pH	Drift and hysteresis low with respect to the high response	n/a	Takechi et al. 2015
Ta$_2$O$_5$ Dual gate ISFET	4 – 9 Commercial pH buffers	402 mV/pH	Relatively stable after 1.5 years of storage	n/a	Kumar et al., 2017
Ta$_2$O$_5$ EGFET	1 – 13 Water + HCl/NaOH Weak effect of monovalent cations	28 mV/pH	<1% drift over 16 min	<10 s	Wu et al., 2017
SiO$_x$ ISFET	2.4 – 11.7 PBS Response is not linear below pH 5. Low effect of varying NaCl concentration.	Up to 14%/pH (drain current normalized to the reference value at pH 7.4)	n/a	Few s	Pfattner et al., 2019

219 **Table 1.** Main characteristics of ISFET based sensors

220 A second family of solid state probes for pH are electrodes based on oxides or metal/metal oxide

221 couples, suitable for a potentiometric sensing setup. Metal/metal oxide pH sensors respond to pH due

222 to an equilibrium involving the metal and its oxide where, in the metal oxide electrodes, the metal is

223 not involved in the potential-determining reaction (Glab et al., 1989).

224 Due to their robustness, relatively easy miniaturization, fast response and good sensing performance,

225 metal/metal oxide and metal oxide materials represent promising substitutes to glass electrodes. pH

226 responsiveness has been observed in many semiconducting oxides, including Sb$_2$O$_3$, PtO$_2$, OsO$_2$,

227 Ta$_2$O$_5$, TiO$_2$, PdO, SnO$_2$, ZrO$_2$, PbO$_2$ and, notably, IrO$_2$ and RuO$_2$ (Hayat & Marty, 2014; Koncki &

228 Mascini, 1997; Yao et al., 2001).

229 Antimony based electrodes have been among the first to be developed and proposed (Kinoshita et

230 al., 1986). As the potential developed by antimony, in response to hydrogen ion activity, is to some

231 degree sensitive to other dissolved anions, the use of a Nafion membrane to cover the electrode has

232 been proposed, resulting in a response stable within 2 mV/pH over 1 month (Xu et al., 2016, 2018,

233 see table 2).

234 Ruthenium oxide is one of the most investigated oxides for pH sensors; its sensing mechanism is

235 attributed to the presence of oxygen vacancies at the surface that lead to the formation of hydroxyl

236 groups by dissociative adsorption of water, generating a pH sensitive layer (Trasatti, 1991). Thick

237 films can be produced by screen printing and 3D structures can be built by the low temperature co-

238 firing of ceramics (LTCC), both industrially scalable processes, showing very high sensitivity and

239 robustness (Manjakkal et al., 2014, 2016; Figure 2). Thick films based on RuO$_2$ containing glass paste

240 by screen printing and sintering; potential was measured against Ag/AgCl in the pH range 2-12 and a

241 linear Nernstian behaviour was observed with a slope of 56 mV/pH. In a formulation with 30 wt% of

242 titania, the sensitivity was maintained at 56.11 mV/pH with a good response time of about 15s and a

243   good 60 days stability. In a similar way, mixed RuO_2/Ta_2O_5 based films were prepared by screen

244   printing and sintering with glass forming oxides. In this case, the response was higher in acid to

245   neutral environment (64.7 mV/pH from 2 to 8) than in basic conditions (43.1 mV/pH from 8 to 11)

246   probably due to the effect of alkaline pH on the supporting glass paste (Manjakkal et al., 2016).

247   Remarkably, in these examples the behaviour of RuO_2 based sensors was not influenced by common

248   anions. However, an influence of oxygen and redox agents has been observed in industrial

249   applications of RuO_2 based sensors. Recently, a double protective layer (Ta_2O_5 thin film and Nafion

250   membrane) has been introduced to mitigate the effect of interfering species (Lonsdale et al., 2018).

251   Some of the reported papers, in the quest for miniaturization and integration of their sensors, propose

252   an integrated solid Ag/AgCl pseudo-reference electrode, to be fabricated into the same substrate as

253   the sensing electrode. The need for a stable reference is, in fact, a key problem for the development

254   of miniaturized solid pH sensors (Hu et al., 2015; Michalska, 2012). We can affirm that a robust and

255   stable alternative to liquid or gel filled electrodes is not yet available, although a number of different

256   designs for disposable and/or reusable solid pseudo-reference electrodes are available (Sophocleous

257   & Atkinson, 2017). The use of modern fabrication technologies can lead to miniaturized multilayered

258   electrodes with stability comparable to traditional ones (Moya et al., 2019).

259   Iridium oxide is also widely employed for pH sensing. It is usually indicated as IrO_x due to its complex

260   stoichiometry, strongly influenced by synthesis conditions (Jang & Lee, 2020). An optimized

261   electrodeposition, followed by an annealing procedure, was developed for the deposition of porous

262   IrO_x films onto gold electrodes (Kim & Yang, 2014). The modified electrodes (Figure 2) showed a

263   nearly perfect Nernstian response to pH changes, with a slope of 59 mV/pH very stable towards cyclic

264   pH changes. Iridium and tantalum oxide thin films were deposited onto platinum electrodes by means

265   of electro-deposition and e-beam sputtering respectively (Uria et al., 2016). Being designed for

266   biological media, these devices were tested in a phosphate buffer saline solution (PBS) within a

267   narrow pH range, resulting in a potentiometric response of 59.4 mV/pH for tantalum and 72 mV/pH for

268   iridium oxide.

269   IrO_x based sensors have good pH sensing performances but their response can be affected by

270   reactions with oxidizing and reducing species dissolved in the test solution. A tantalum oxide layer

271   deposited over IrO_x has been tested as a barrier layer, increasing the stability of the signal against

272   oxygen (Kuo et al., 2014). Recently, a further refinement in the oxidation procedure of iridium wires

273   led to the production of a remarkably stable sensor, with no need for barrier layers (Pan et al., 2018).

274   This sensor was tested in the presence of a large set of anions and cations and in marine water,

275   exhibiting stability and sensing performances in line with the glass electrode used as a reference. A

276   very similar $Ir/Ir(OH)_x$ pH electrode has been recently fabricated and field tested in seawater,

277   comparing the results with a commercial pH meter (Zhang et al., 2017). The solid state electrode

278   showed good stability (137 days) and a precision comparable to the reference glass sensor, with a life
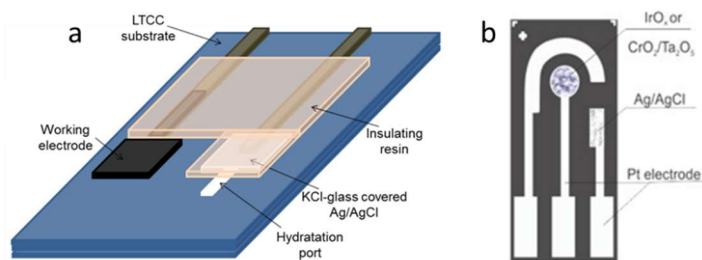
279   span up to 5 months.

Figure 2. Assembly of: sintered RuO_2 working electrode onto LTCC ceramic substrate (a) (Reprinted from Manjakkal et al. (2016), with permission from Elsevier); gold electrode modified by electrodeposited IrO_x (b) (Reprinted from Uria et al. (2016), with permission from Elsevier). Both solutions include a pseudo-reference solid Ag/AgCl electrode.

Other metal oxides used for pH measurements include WO_3, TiO_2, ErO_2 and MnO_2. Manganese oxide was shown to exhibit a non-linear electrical response to pH (and a tendency to dissolve in acidic solutions) due to the chemical equilibrium among the oxide and the oxo-hydroxide species. A microelectrode was fabricated by coating MnO_2 with a polymeric proton-conductive Nafion membrane, showing a linear response in the 4 – 12 pH range with a slope of 60 mV/pH (Cachet-Vivier et al., 2010). In a recent study, a tungsten bronze with a well-defined composition and crystal structure was produced by oxidation of tungsten wire and has been proposed as electrode material for potentiometric pH detection (Cisternas et al., 2017). The response of this material was found to be highly reproducible and stable (variations in the order of 0.3 mV) upon storage and continuous operation conditions. The use of multiple metals in a single device has been investigated by Sadig et al. (2018) that realized an iridium, ruthenium and titanium oxide based tri-oxide system. Though no details are given on the structure of the deposited oxide layer, the response recorded showed a linear potential/pH relation whose slope was stable within 0.3 mV over 120 days of testing. Finally, it is worth reporting on the design of a sensor based on solid metal rods, expressly developed for seawater monitoring (Brooke et al., 2016). To overcome the interefences of corrosion, surface reactions and fouling, 8 different metals were simultaneously used and their potential against a common zinc counter electrode was recorded continuously against pH, measured by a reference pH meter, allowing the calibration of the device through a self-learning neural network algorithm. After calibration, the device was able to reproduce actual pH values over 3 weeks of deployment.

Sensing material and setup	Testing range and media	Sensitivity	Stability	Response time	Reference
Sb_2O_3 – Nafion membrane Potentiometric	4 – 9 Commercial buffers	54.5 ± 2 mV/pH	Stable within 2 mV/pH over 1 month (measurement repeated every week)	20 s	Xu et al., 2018
RuO_2/TiO_2 Potentiometric	2 – 12 HCl/NaOH solutions. Interference of Li^+, Na^+ and K^+ negligible	56.11 mV/pH	Storage in ambient condition up to 2 months with no change in properties	15 s	Manjakkal et al., 2014
RuO_2/Ta_2O_5 Potentiometric	2 – 12 HCl/NaOH solutions and H_3BO_3/citric	64.7 mV/pH (pH 2–8)	Storage in ambient conditions up to 2 months led to a	15 s	Manjakkal et al., 2016

	acid/Na_3PO_4 buffer. Interference of Li^+, Na^+ and K^+ negligible	43.1 mV/pH (pH 8–11)	small reduction in sensitivity.		
IrO_x Potentiometric	2.4 – 11.6 Commercial buffers	59.5 mV/pH	n/a	2 s	Kim & Yang, 2014
Ta_2O_5 / IrO_x Potentiometric	3 – 8 PBS acidified with HNO_3 Chloride ion concentration can influence reference stability.	59.4 mV/pH (Ta_2O_5) 72 mV/pH (IrO_x)	Stable after incubation in LB/ glucose for 24h.	Few s	Uria et al., 2016
IrO_x Potentiometric	2 – 13 Britton – Robinson buffer Good selectivity against common cations	59.5 mV/pH	Drift < 0.1 mV/h	n/a	Kuo et al., 2014
$Ir(OH)_x$ carbonate oxidized Potentiometric	2 – 10 Commercial buffers **Tested in seawater (pH 7.9)** Negligible effect of common cations anions and O_2	56.8 – 57.6 mV/pH	No drift over 48 h at pH 6.	1 s	Pan et al., 2018
$Ir(OH)_x$ Potentiometric	4 – 9 Calibrated in commercial buffers**Tested in Dickinson seawater (pH 7.876) and in open sea**	56.1 – 59.5 mV/pH	Negligible drift over 200s. Stable during 137 d of continuous recalibration in standard buffers	5 s	Zhang et al., 2017
MnO_2 – Nafion membrane Potentiometric	2 – 12 H_2SO_4/NaOH solutions Interference by Fe^{2+} ions.	≈ 60 mV/pH	n/a	35 to 74 s	Cachet-Vivier et al., 2010
$Na_{0.75}WO_3$ Potentiometric	1 – 10 Commercial buffers, KCl/HCl solution (pH 1) High selectivity against Na^+ K^+ Mg^{2+} Ca^{2+}	≈ 56 mV/pH	Stable for storage in air up to 6 months and for repeated measurements over 1 w	13 – 18 s (depending on pH)	Cisternas et al., 2015; Cisternas et al., 2017
IrO_2-RuO_2-TiO_2 Potentiometric	1 – 13 Tris buffer Some influence of K^+ ions	59 mV/pH	Stable for 120 d	4 – 8 s	Sadig et al., 2018
Stainless Steel, Cu, WC, Brass, Ni, Al, Ti, Bronze Potentiometric vs a common Zn counter-electrode	**Tested in seawater**	Neural network calibration correlates potential readings with pH	Signal degradation after 1 month of deployment	n/a	Brooke et al., 2016

Table 2. Main characteristics of metal/metal oxide based sensors. In bold, sensors that have been tested in seawater.

Metal oxide based pH sensors are finding increasing popularity due to their ruggedness and relatively low price. However, most of the prospective applications are not demanding, in terms of accuracy and stability, like seawater monitoring.

309   There are interesting examples of metal oxide sensors tested in seawater. Zhang et al. (2017)

310   integrated four IrO_x pH electrodes and one Ag/AgCl reference electrode in a self-made chemical

311   sensor, and deployed it in a profile detection of nearly 70 m for a sea trial, near Newport Harbor,

312   California. The pH value measured by the sensor was very close to the data given by a Sea-Bird 911

313   plus CTD, taken as a reference (maximum deviation 0.06 pH units), with the IrO_x sensor showing a

314   better data matching in the 0–40 m water depth range. The sensors were subjected to periodic

315   calibrations for a 137 days period, showing a remarkable response stability. The authors contend that

316   the high precision and accuracy of the sensor make it possible to use in the ocean observation field.

317   Pan et al. (2018), fabricated an IrO_x based electrode, whose response to pH was tested in various

318   buffers and in seawater samples. Their sensors showed a good agreement (maximum deviation 0.04

319   pH units) with a commercial glass electrode in all testing conditions, showing a remarkable selectivity

320   against interfering ions. No data is available for long term deployment in seawater.

321   Furthermore, Brooke et al. (2016) described the simultaneous use of eight metal electrochemical cell

322   for measuring ocean pH through a non-linear calibration algorithm obtained using a neural network

323   self-learning approach. A prototype sensor was deployed in a seawater tank at the Seattle Aquarium

324   for one month and, after the calibration period, was able to reproduce pH values within 0.02 pH units

325   vs. the reference pH electrode for up to 3 weeks, before corrosion and fouling started to affect the

326   response.

327   The latest developments in the field of inorganic films, for both FET and potentiometric pH sensing

328   devices, are directed towards the fabrication of nanostructured/multilayer electrodes with improved

329   performances and reduced cost. These approaches will be treated in Section 5.

330

4. Polymer-based pH sensors

331

332   Polymer based materials, in particular conducting polymers, are finding ever increasing applications in

333   the sensing field, due to their versatility, low cost and robustness (Adhikari & Majumdar, 2004).

334   A general feature of conducting polymers is their "redox" activity and, as a consequence, the

335   possibility to change their electrical behaviour (charge carrier density, band structure) through a

336   doping-dedoping effect generated by the interaction with ions or small molecules (Adhikari &

337   Majumdar, 2004; Culebras et al., 2014). These interactions constitute the basis for the use of

338   conducting polymers for sensing (Gupta et al., 2004; Persaud & Pelosi, 1985).

339   Huang et al. (1986) investigated in detail the effect of pH on conducting polymers, in particular

340   polyaniline (PANI) and showed that the pH influences the redox processes of PANI in aqueous

341   electrolytes. Since the first pioneering studies, the most investigated polymers in sensing have been

342   polythiophene, polypyrrole (Ppy) and, notably, polyaniline and its derivatives, deposited or

343   polymerized directly onto metal electrodes.

344   Doped PANI can be produced by electrochemical polymerization of aniline in the presence of

345   tetraphenyl borate (Pandey & Singh, 2001). The potentiometric measurement carried out in buffers

346   and electrolytic solutions showed a linear potential/pH relationship, and a claimed stability of 6 months

347   (Table 3). However, a super-Nernstian response was observed, attributed to a non equilibrium

348   protonation/deprotonation process. In a more complex design, a graphite lead was covered with in

349   situ polymerized PANI (Gao & Song, 2009) and used for amperometric sensing of pH in the range 1.8

350   – 9.9. The voltammetric I/V curve shifted towards negative potential with increasing pH, showing a

351   bilinear correlation and high reproducibility (0.5% error on repeated measurements). The higher slope

352   recorded in the acidic range was attributed to multiple oxidation states possible for PANI. Recently,

353   disposable and low cost sensors were realized by drop casting a PANI solution on carbon electrodes,

354   printed on a paper substrate. Ag/AgCl solid pseudo-references were produced on the same substrate

355   to fabricate an integrated device that showed a linear response to pH in the range 4 – 10, stable

356   during 24h (Rahimi et al., 2016). Flexible interdigitated electrodes deposited on a polyimide film

357   (Figure 3) have been covered by spin casting with a PANI film, doped with dodecyl benzene sulfonic

358   acid (Li et al., 2020). The flexible sensors were calibrated in phosphate buffers and showed a linear

359   potential response vs. pH up to pH 8.6.

360   Platinum electrodes, realized by photolithography, have been modified with polypyrrole and used by

361   Lakard et al. (2007); the potentiometric response of these sensors was tested in the pH range 2 – 11,

362   showing a nearly linear dependence of potential with pH. The sensitivity, however, showed a

363   progressive decrease over 30 days of monitoring, attributed to the degradation of the silver pseudo-

364   reference electrode. Ppy polymerized onto PEI modified electrodes showed improved stability, due to

365   the adhesion granted by the imine layer (Segut et al., 2007). As a more recent example of a

366   potentiometric sensor made by electropolymerization, it is worth mentioning the device proposed by

367   (Li et al., 2011). By polymerization of bisphenol A (BPA) onto ITO glass, the authors developed an

368   electrode that was tested in either potentiostatic or potentiometric setup, in a wide pH range (1 to 14)

369   showing a sensitivity close to the Nernst limit and a reasonable stability of the response up to 12
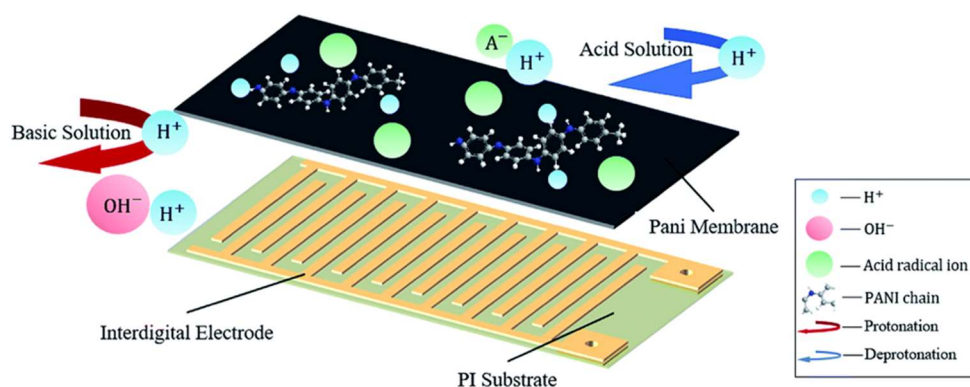
370   days.

372   **Figure 3.** Schematic representation of an interdigitated gold electrode with deposited PANI sensing layer
373   undergoing reversible protonation/deprotonation. Reproduced from Li et al. (2020) - Published by The Royal
374   Society of Chemistry.

375   Recently, a non-conjugated, redox active polymer, poly(dopamine), demonstrated a linear correlation

376   of the redox peak measured by voltammetry with pH. The polymer was deposited on a carbon

377   electrode and tested in a wide pH range, in different buffers or saline solutions showing an excellent

378   stability of the response (Amiri et al., 2016).

Combinations of conducting polymers with support polymers have been also realized by various methods, including the deposition of preformed polymer from solutions, reducing the cost of the assembly and overcoming the difficulties of electrodeposition. Gill et al. (2008) developed a composite conductimetric pH sensor mixing doped PANI particles with polyvinyl butyral and polypyrrole. The composite was deposited by screen printing on an interdigitated electrode and showed a linear response to pH in the range 2 – 8, but a response time of about 200 s. An analysis of the sensor response as a function of composition revealed that PANI is the active component while polypyrrole contributes to increase the system conductivity. As a development of this concept, a gel with similar composition was tested for the real time detection of pH in drinking water (Banna et al., 2014). Gold interdigitated electrodes were covered with the sensitive polymers and exposed to solutions in the pH range 6.5 – 9 showing a non-linear change in resistivity that was stable over 30 days of continuous exposure. The accuracy and resolution of this sensor were similar to commercial devices.

Sensing material and setup	Testing range and media	Sensitivity	Stability	Response time	Ref.
PANI/ tetraphenylborate Potentiometric	2 – 9 Tris-HCl buffer Negligible effect of Na^+, K^+, Ca^{2+}	≈ 86 mV/pH	Stable after 6 months storage	n/a	Pandey & Singh, 2001
PANI Amperometric	1.8 – 9.9 Britton-Robinson buffer	32.4 mA/pH (pH 1.8 – 5.5) 15.9 mA/pH (pH 5.5 – 9.9)	0.5% error on consecutive measurements	5 s (85% of reading)	Gao & Song, 2009
PANI Potentiometric	4 – 10 Commercial buffers	50 mV/pH	Drift ≤ 0.01 pH/h during 24h	12 s	Rahimi et al., 2016
PANI Potentiometric	5.45 – 8.62 Phosphate buffer	58.6 mV/pH 2.4% standard deviation	Hysteresis < 12% of full scale	54 s	Li et al., 2020
PEI / Ppy Potentiometric	4 – 9 Commercial buffers. Interference of carbonate ions	≈ 50 mV/pH Dependent on film structure	Slight decrease of sensitivity over 30 d	<60 s	Segut et al., 2007
Poly(bisphenol A) Potentiostatic/ Potentiometric	-1 – 15 50nM NaCl + HCl or NaOH. No effect of Na^+, K^+, Cl^-, SO_4^-	58.6 ± 1.4 mV/pH (Potentiostatic) 56.7 ± 1.6 mV/pH (Potentiometric)	Stable within ≈ 4% after 12 d of storage.	20 s	Li et al., 2011
Poly(dopamine) Potentiostatic	1 – 12 Phosphate, acetate, carbonate, Britton-Robinson buffers. HCl/KCl solution	58.2 mV/pH	Stable within 0.8% for repeated measurement. Slight effect of buffer ionic strength, corrected by calibration	n/a	Amiri et al., 2016
PANI/ Ppy in poly(vinyl butyral) gel Conductometric	6.4 – 9 Tap water	Non-linear resistivity/pH calibration curve.	Precision 0.07 pH units. Stable for 30 d of continued use	n/a	Banna et al., 2014

Table 3. Main characteristics of polymer based sensors.

393 Polymer based pH sensors, mainly based on organic conductive polymers, have been known for a

394 long time. Many different designs and compositions have been proposed, but their development has

395 been limited up to now to lab scale studies. This fact can be due to the low compatibility of polymer

396 processing conditions with the traditional electronic technologies that rely on inorganic

397 semiconductors and oxides. Moreover, the relatively low stability of polymer electrical response may

398 have contributed to the low diffusion of polymeric sensors for pH monitoring. Nevertheless, the

399 popularity of polymer based sensors is now increasing, following the development of flexible, printable

400 organic electronics, and polymers can be the ideal candidates for the fabrication of disposable

401 devices with short service life. In the most recent researches, conductive polymers are combined with

402 nanomaterials for enhanced sensitivity, response time and selectivity (Ates, 2013).

5. Nanomaterial-based sensors

404 The continuous quest for high sensitivity, fast response time, flexibility and cost-effectiveness is the

405 driving force for the research of new solutions and materials for sensing. The use of nanoscale

406 materials, both organic and inorganic in the realization of sensing devices, has been recently

407 proposed leading to very interesting improvements in sensor performances (Salavagione et al., 2014).

408 The first and more obvious consequence of the structuring at very small length scale, is the large

409 increase in surface area. As the interactions with probe solutions are usually limited to the surface of

410 the sensing material, this leads to an immediate increase in sensitivity that allows the design of

411 miniaturized devices with weight, energy and cost savings.

5.1 Organic and carbon-based nanomaterials

413 One-dimensional nanomaterials based on conducting polymers can be fabricated using well-

414 established wet chemical techniques and their properties can be easily tuned during synthesis or with

415 a doping step. Nanotubes and nanowires with enhanced sensitivity toward various chemical/biological

416 species are then ideal candidates for the design of new sensors (Bangar et al., 2010).

417 Nanowires fabricated with different methods have been proposed for the realization of pH sensing

418 devices. Shirale et al. (2010) fabricated a FET sensor based on a single PPy nanowire for real-time

419 pH monitoring and examined how the diameter of the nanowire affects the sensor performance. The

420 sensor showed a linear correlation of the drain current with pH in the range 1 – 11 (Table 4). Doped

421 Ppy nanowires were fabricated by electropolymerization on a gold substrate (Sulka et al., 2013). The

422 gold/Ppy electrode was then used as a potentiometric sensor in buffer solutions, in the pH range 2 –

423 12: it was shown that the oxidizing agent used for the polymerization influences the response, with

424 $LiClO_4$ giving the best sensitivity (49.3 mV/pH). Remarkably, the nanowires showed a ten-fold

425 increase in sensitivity compared with thin films of Ppy prepared in the same conditions.

426 Recent developments in polymer based pH sensors are generally directed towards the realization of

427 flexible devices, as an example, by printing carbon based electrodes onto plastic films and modifying

428 them with active materials. PANI nanofibers directly polymerized at the surface of carbon electrodes

429 supported on PET were tested at pH between 4 and 10 (Park et al., 2019). The Nernstian response

430   was observed with good repeatability (97.9%) and reasonable stability (drift of 3 mV/h over 15 h). An

431   interesting flexible pH sensor was fabricated by soft-lithography templating of nanopillars on a

432   polyurethane/acrylate layer followed by electrodeposition of polyaniline (Figure 4). A solid Ag/AgCl

433   pseudo-reference electrode was deposited as a reference and the sensor was tested in the 2 – 12 pH

434   range, showing a remarkably fast (≈ 1 s) and accurate response (compared to a reference glass

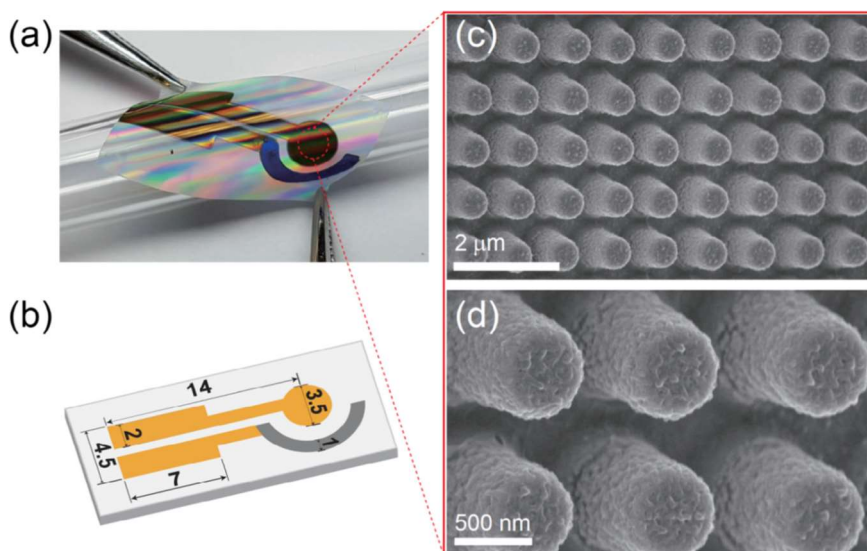435   electrode) even in complex samples like juices and coffee (Yoon et al., 2017).

436

437   **Figure 4.** Templated nanopillars realized by soft lithography and flexible electrode assembly (Journal of Colloid

438   and Interface Science 490 (2017) 53–58). Reprinted from Yoon et al. (2017), with permission from Elsevier.

439   Dodecyl benzene sulfonic acid doped PANI nanoparticles were conveniently incorporated into an

440   epoxy resin to produce thin films for conductometric measurement of pH in soil (Patil et al., 2019).

441   The films showed a high conductivity when loaded with 10 wt% of PANI and were tested in

442   commercial buffers showing a good linearity of relative conductance vs. pH.

443   Carbon nanotubes (CNTs) and graphene (G) are among the most investigated nanomaterials for

444   sensing applications, thanks to their unique chemical structure, very high conductivity, chemical

445   stability and high surface area (Chen et al., 2011; Martin & Escarpa, 2014).

446   Ideal graphene (G) is a single layer of sp^2 carbons arranged in a hexagonal structure extended in 2

447   dimensions (Li et al., 2009; Novoselov et al., 2012). Carbon nanotubes are tubular structures ideally

448   formed by rolling up one (single-wall, SWCNT) or more (multi-wall, MWCNT) graphene sheets. The

449   surface chemistry of carbon nanostructures can be tuned by the introduction of specific chemical

450   groups, influencing their electronic and chemical behaviour (Ramanathan et al., 2008; Tasis et al.,

451   2006). Graphene derive materials known as graphene oxide (GO) and reduced graphene oxide (rGO)

452   are interesting alternatives to graphene, showing higher reactivity at the expense of conductivity.

453   An interesting report on the correlation of CNT conductivity with pH was published in (Lei et al., 2012).

454   The authors simply deposited a layer of multiwall CNTs onto filter paper and then showed a nice

455   correlation of the system resistivity with pH of buffer solutions. Similarly, the pH response of graphene

456   was observed on a simple resistive device, by deposition of exfoliated graphene onto a silicon wafer.

457   Platinum electrodes were then deposited and the resistivity measured showed a linear correlation with

458 pH that was explained by an n- and p-doping effect induced by H$^+$ and OH$^-$ ions respectively (Lei et

459 al., 2011). A number of studies show that the electrical response of graphene and CNTs exposed to

460 aqueous electrolyte solutions depend on various interfering factors (pH, dissolved ions, substrate

461 surface, Heller et al., 2010) and that the formation of charges at CNT or graphene surfaces is mainly

462 driven by the presence of "defects" (Back & Shim, 2006), such as oxidized groups (Tan et al., 2013).

463 This findings are in line with papers reporting a negligible sensitivity to pH for perfect, defect free

464 graphene sheets (Fu et al., 2011). Summarizing, a consistent explination of the pH response of

465 carbon nanomaterials is still lacking.

466 Recently, ink-jet printing was used to deposit –COOH functionalized SWCNTs on glass and polymeric

467 substrates, obtaining a potentiometric sensor. A linear response, with slope related to the number of

468 layers, was recorded in the pH range 3 – 11 (Qin et al., 2016). Carbon nanotubes can also be

469 integrated into traditional semiconductor-based electronics for the realization of transistor-like devices

470 with sensing properties. An extended gate FET (EGFET) was realized with a CNT network (Chien et

471 al., 2012) employed for both the contact electrode and the sensing membrane. The CNTs were first

472 acid-oxidized and then irradiated with a laser beam to increase the defect concentration on their

473 surface. This treatment resulted in a greater sensitivity)50.9 mV/pH) of the FET to pH and in a good

474 linearity (Correlation coefficient R^2: 0.998) of the response.

475 Similarly, most graphene based sensors are, realized as transistors. Ohno et al. (2009) reported on

476 the fabrication of a solution-gated FET (SGFET) made by a single layer of mechanically exfoliated

477 graphene onto SiO$_2$/silicon substrate. The charge transport properties of the graphene layer depend

478 on pH and a nearly linear correlation was found between the gate potential (measured at the Dirac

479 point) and pH, with a sensitivity of approximately 30 mV/pH. For the same kind of device (Ohno et al.,

480 2010), the authors analyzed the signal/noise parameters in a narrower pH range (5 – 8) and

481 calculated a promising detection limit of 0.025. Using a different approach, few-layer graphene

482 (thickness 1-2 or 3-4 layers) was grown epitaxially on silicon to realize a SGFET, tested in the pH

483 range 2 – 12. Interestingly, a super-Nernstian sensitivity of 99 mV/pH was recorded, irrespective of

484 the thickness (Ang et al., 2008). The authors performed impedance spectroscopy to rule out any

485 external influence on the conduction behaviour of the device, demonstrating that only the adsorption

486 of OH$^-$ / H$_3$O$^+$ species determines the properties.

487 One of the interesting advantages of carbon nanomaterials is the possibility to use conventional

488 fabrication techniques to realize electronic devices and sensors on flexible substrates (Jung et al.,

489 2014; Sharma & Ahn, 2013). Single wall nanotubes were employed for the fabrication of flexible FETs

490 supported on polyethylene terephthalate (PET) films, using a layer-by-layer (LbL) approach. The film

491 was obtained by LbL deposition of carboxylated SWCNT with two polyelectrolites, to work as the gate

492 electrode. The response of the FET was found to be dependent on pH, although in a non-linear way

493 (Lee & Cui, 2010). Mailly-Giacchetti et al. (2013) transferred graphene layers, grown by CVD, onto

494 poly(ethylene 2,6-naphthalenedicarboxylate) (PEN), silicon modified with octadecyltrichlorosilane

495 (OTS) and SiO$_2$, to evaluate the influence of the substrate on sensing. Although the different devices

496 showed different conductivities, the sensitivity to pH was around 22 mV/pH for all of them.

497 Some refinements in the design of graphene devices have been proposed to improve the sensing

498 performances. A suspended graphene FET was fabricated with a claimed increase in the signal to

499 noise ratio by 14 dB with respect to the same unsuspended device (Cheng et al., 2010). The increase

500 in signal quality allowed measurements to be carried out with very low applied voltage, reducing the

501 risk of interference from the testing solution (polarization, redox reactions). An interesting approach to

502 increase the contact surface with the aqueous solution has been recently proposed by Ameri et al.

503 (2016) with the realization of a high porosity graphene foam covered by a thin layer of HfO_2. This

504 device was tested in Dulbecco phosphate buffer, showing a super Nernstian sensitivity of 71 mV/pH

505 and a fast response. Finally, a solid gated G-FET designed to avoid the need for an external

506 reference electrode has been reported. In this device, a layer of HfO_2 is deposited between the

507 graphene layer and a gold gate electrode (Zhu et al., 2015). The response of the FET was linear with

508 pH in the range 5.3 – 9.1, with a sensitivity of 56.5 mV/pH.

509 GO and rGO materials can be used for the fabrication of membranes and networks, showing lower

510 electrical properties compared to graphene but good pH sensitivity, probably due to the high

511 concentration of oxidized groups (Sohn et al., 2013). A potentiometric GO based sensor has been

512 realized for medical applications by printing the electrodes on a plastic substrate (Salvo et al., 2017)

513 and calibrated in a buffer with isotonic salt concentration. The potential response to pH was linear and

514 the sensors proved to be relatively stable for 1 week in serum. A sensor for seawater pH detection

515 was derived from this system (Poma et al., 2019) and validated in high ionic strength buffers and real

516 seawater. GO and rGO electrodes were coated with Nafion to increase stability and tested, with rGO

517 (functionalized with 4-aminofenilacetic acid) showing the highest sensitivity. Stability was assessed for

518 up to 8 days in seawater but the accuracy of the sensor was worse than the reference glass

519 electrode.

520 Nanomaterials are often combined with polymeric substrates/matrices, for processing reasons and to

521 enhance sensing performances by exploiting the synergism between the components. Synergistic

522 effects can be observed in carbon nanomaterials combined with conducting polymers: the polymer

523 increases the robustness and selectivity of the response; at the same time, the incorporation of

524 nanoparticles improve the stability and the conductivity of polymers, enhancing the electric properties.

525 Polyaniline is by far the most studied conducting polymer for the development of composites (Oueiny

526 et al., 2014). Interesting results have been obtained by Loh et al. (2007), by combining CNTs with a

527 conducting layer-by-layer thin film of PSS/PANI and employing the assembly in a resistive pH sensor.

528 The electrical resistance showed a large shift upon pH change (pH 1 to 10), with a sensitivity of

529 approximately 19.9 kΩ cm^{-2}/pH. Similarly, Boeva et al. (2014) produced few-layer graphene and

530 exfoliated (30 – 50 layers) graphite coated by PANI. The redox behaviour of these materials was

531 investigated by cyclic voltammetry, showing that PANI nanocomposite preserve their electroactivity up

532 to neutral pH due to interactions with the graphene, whereas neat PANI loses its conductivity above

533 pH 3. A miniaturized pH meter based on amino-functionalized graphene/PANI nanocomposite was

534 fabricated by electropolymerization on ITO/glass substrate and tested by voltammetric measurements

535 in PBS buffer, resulting remarkably stable up to pH 11 (Su et al., 2016). Similarly, a good sensing

536 performance was also recorded on polyaniline functionalized rGO, tested in both potentiometric and

537 resistive setup in the range 2 – 9. The PANI-rGO electrodes were coated with a Nafion film to
538 decrease interference from other ions and tested in a L. Lactis fermentation reactor (Chinnathambi &
539 Euverink, 2018). Recently, Grozdanov et al. (2018, 2019) have tested screen printed electrodes
540 (SPE) modified with PANI/carbon nanotubes composites as pH nanosensors, in the frame of FP7
541 project COMMON SENSE (Cleary et al., 2014; Barton et al., 2016; Ribotti et al., 2015). Nanosensors
542 were prepared by electropolymerization and exhibited a high value of conductivity, which was
543 attributed to the synergistic effect of the conductive polymer and carbon nanostructure via π-π
544 stacking. Conductivity changes were measured at different pH (4 to 10) in commercial buffers, as well
545 as in seawater samples showing a non linear response to pH. Similar electrodes were produced by
546 Bao et al. (2019), who produced a PANI/MWCNT ink for screen printing of miniaturized working
547 electrodes. Here, the response was measured by chronoamperometry, observing a linear relationship
548 of potential vs. pH in the range 2 – 11; the role of nanotube/PANI interactions in the enhancement of
549 the electric response was pointed out. Amperometric pH sensors were produced (Sha et al., 2017) by
550 electropolymerization of well-ordered PANI chains on graphene-modified carbon electrodes, showing
551 a nearly linear response to pH. The sensitivity was higher in alkaline solutions, which is rarely
552 observed for PANI due to the dependence of electroactivity on acid doping.

553 A number of other polymers have been used for nanocomposite sensors fabrication. Gou et al.
554 (2014). deposited a layer of oxidized SWCNTs between gold electrodes onto a silicon substrate, then
555 poly(1-amino anthracene, PAA) was electropolymerized onto CNTs. The obtained device was tested
556 in either liquid gated FET or conductometric configuration in various pH, showing high sensitivity and
557 stability of the response over long time. The detection limit (resolution) is 0.04 pH. Recently, a
558 biomimetic polymer, polydopamine (PDA), has also shown redox properties (Amiri et al., 2016) and,
559 thanks to its excellent adhesion properties, has been used to modify nanostructured carbon
560 electrodes (Figure 5; Zuaznabar-Gardona & Fragoso, 2018). PDA response was investigated by both
561 cyclic voltammetry and potentiometry, showing a higher sensitivity when combined with carbon
562 nanostructures, up to 53 mV/pH. The electrodes were stable for several months in water and only
563 attacked by strong alkaline solutions. They were also tested in seawater showing a very good
564 agreement with the reference pH meter.
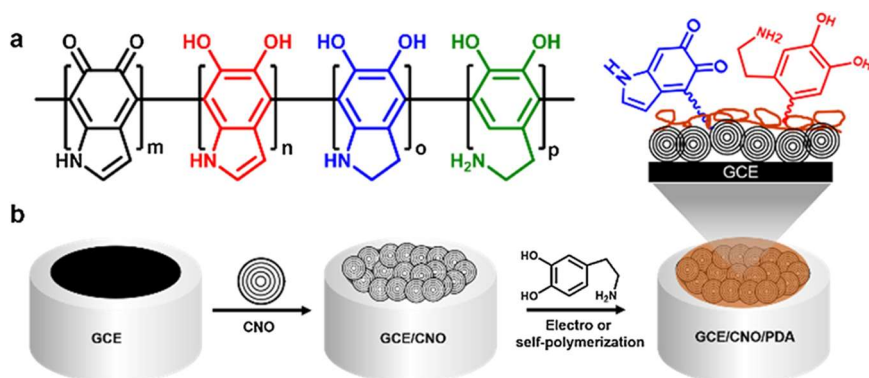
565

566 **Figure 5.** General structure of polydopamine (a) and schematic fabrication of nano-onions (CNO) and
567 polydopamine (PDA) deposition on glassy carbon electrodes (GCE) (b). Reprinted from Zuaznabar-Gardona and
568 Fragoso (2018), with permission from Elsevier.

As a further example of polymer/nanoparticle synergism, it is worth mentioning the design proposed by Crespo et al. (2009). An acrylic ion selective membrane, doped to increase the selectivity towards H^+ ions, was casted on a MWCNT-modified carbon electrode and tested for potentiometric pH measurements. Nanotubes here are introduced as a solid contact between the polymeric membrane, exhibiting pH dependent ionic conduction, and the working electrode. The result is a sensor with Nernstian response and good selectivity. The design of this kind of sensor has been refined over the years leading to the fabrication of a complete apparatus for field testing campaigns in freshwater (Athavale et al., 2017) and, notably, in seawater (Cuartero et al., 2017) showing performances comparable with commercial sensors.

Sensing material and setup	Testing range and media	Sensitivity	Stability	Response time	Reference
Polypyrrole NW ISFET	1 – 11 Commercial buffers	0.4/pH (normalized drain current)	n/a	Few s	Shirale et al., 2010
Polypyrrole NW array Potentiometric	2 – 12	Up to 49.3 mV/pH	Stable up to 50 d of storage	n/a	Sulka et al., 2013
PANI nanofibers Potentiometric	3 – 10 Commercial buffers Good selectivity against common cations	62.4 mV/pH	Drift of 3 mV/h over 15h	12.8 s	Park et al., 2019
PANI nanopillars Potentiometric	2 – 12 Commercial buffers Negligible effects of of Na^+, K^+, $NH4^+$, Ca^{2+}, and Mg^{2+} at 10 mM	60.3 mV/pH	Low drift (0.64 mV/h) during a 15h test	5 s	Yoon et al., 2017
PANI particles in epoxy Resistive	2.4 – 10 Commercial buffers	957 µS/pH	Stable within 4% for 30 d (tested every 5 d)	5 – 30 s	Patil et al., 2019
SWCNT-COOH Potentiometric	3 – 11 Britton-Robinson buffer	48.1 ± 0.4 mV/pH	Response is reduced by 4% after 15 d of storage	7 s	Qin et al., 2016
MWCNT-COOH EGFET	3 – 13 PBS	50.9 mV/pH	n/a	n/a	Chien et al., 2012
Single graphene layer on SiO_2 Solution gated FET	4 – 8.2 10 mM phthalate, phosphate and borate buffers	Approx. 30 mV/pH Resolution is 0.025 pH units	n/a	n/a	Ohno et al., 2009, 2010
Single graphene layer on PEN Solution gated FET	4 – 9 Phosphate buffer adjusted with strong acids/alkali	22 mV/pH	Response decrease after exposure to acid solutions	≈ 10 min	Mailly-Giacchetti et al., 2013
Graphene foam coated with HfO_2 Solution gated FET	3 – 9 Dulbecco buffer adjusted with strong acids/alkali	71 ± 7 mV/pH	n/a	≤ 240 s	Ameri et al., 2016
Graphene + HfO_2 dielectric layer FET	5.3 – 9.2 Phosphate saline buffer	56.5 mV/pH	n/a	< 60 s	Zhu et al., 2015

rGO Solution gated FET	6 – 9 Phosphate buffer	29.2 mV/pH	n/a	Few s	Sohn et al., 2013
GO Potentiometric	4 – 10 Citrate, borate, phosphate buffers (isotonic) Tested in human serum	40 ± 4 mV/pH	Negligible drift over 1 h in buffers. Stable for 1 w in serum	n/a	Salvo et al., 2017
Reduced GO + Nafion membrane Potentiometric	4 – 10 Citrate, borate, phosphate **Tested in superficial seawater.**	45 mV/pH	Fluctuations observed in the response over 56h in buffers. Signal stable for 8 d in seawater	n/a	Poma et al., 2019
Graphene platelets Resistive	1 – 10 Commercial buffers	19.9 (kΩ/cm^2)/pH Poor linearity	n/a	n/a	Loh et al., 2007
Amino functionalized graphene / PANI Voltammetry	1 – 11 PBS	51.1 mV/pH	Response decrease after 1 w	n/a	Su et al., 2016
rGO/PANI + Nafion membrane Potentiometric Resistive	2 – 9 Britton-Robinson buffer Also tested in a bacterial fermentation broth	55 mV/pH 1.71 Ω/pH	n/a	n/a	Chinnathambi & Euverink, 2018
PANI-MWCNT Chronoamperometry	2 – 11 Water adjusted with HCl/NaOH	20.6 mV/pH	n/a	Few s	Bao et al., 2019
PANI on graphene-carbon electrode Amperometric	1 – 11 NaCl solution adjusted with HCl, H$_3$PO$_4$, NaOH	50.17 μA /(pH cm^2) for pH 1 – 5 139.2 μA /(pH cm^2) for pH 7 – 11	n/a	$\approx$ 100 s	Sha et al., 2017
SWCNT – PAA Solution gated FET / Conductometric	2 – 12 Britton-Robinson buffers Response to Na$^+$ and Ca$^+$ negligible	0.073 mS/pH	Stable for $\approx$ 2 h (no drift). Same sensitivity after 120 d of storage.	$\approx$ 60 s	Gou et al. 2014
Polydopamine/carbon nano-onions Potentiometric	1.5 – 10.5 Universal buffer **Tested in seawater (pH 8.3)** Low interference of alkaline cations	53 mV/pH	Stable over 4 w	15 s	Zuaznabar-Gardona & Fragoso, 2018
MWCNT solid contact + acrylic membrane Potentiometric	3 – 10 Various buffers Lake freshwater **Tested in seawater (pH 7.9 – 8)** Selective against alkali cations and sulfides	58.8 ± 0.4 mV/pH	Estimated drift 0.1 mV/h.	10 s	Athavale et al., 2017; Cuartero et al., 2017

578   **Table 4.** pH sensors based on nanostructured polymers, carbon nanomaterials and their combination. In bold,
579   sensors that have been tested in seawater.

580   Three of the pH sensors listed in Table 4 have been recently tested in seawater, while most of the
581   published works on sensors based on carbon-based nanomaterials only tested the sensors in
582   buffered solutions. The first consists of a graphene-based pH sensor, part of an autonomous system
583   for the remote monitoring of pH and temperature at sea (Poma et al., 2019); the pH measurement is
584   performed through a potentiometric sensor with a wireless, smartphone-based real time acquisition
585   system. The pH sensor was initially validated in the laboratory at controlled temperatures and in water
586   previously collected at sea. Then it was left at sea with a sampling rate of one measurement per hour
587   for 8 days. In both cases, a commercial glass electrode pH-meter was used as a reference device.
588   Laboratory and on-field results have shown the great versatility of such a low cost system, providing
589   pH values comparable with commercial sensors but with a lower energy consumption and a greater
590   calibration stability. The second pH sensor is again potentiometric like the first one but based on
591   polydopamine (PDA) films coated on a carbon nano-onion conductive surface. Also in this case, the
592   new pH sensor was validated through comparison with a commercial combined glass pH electrode
593   coupled to a pH meter from the same builder in water sampled at sea. They showed an excellent
594   correspondence between these new PDA pH sensors and commercial ones with the advantages of
595   an easy fabrication, an excellent reproducibility, a stability of the PDA coating in water over several
596   months and the possibility of its integration into miniaturized devices. Both the potentiometric pH
597   sensors described above must be tested in the field for longer times in order to verify stability and the
598   long term effects e.g. of biofouling on system performances. The last example of a potentiometric
599   sensor successfully tested in freshwater (Athavale et al., 2017) and in seawater (Cuartero et al.,
600   2017), is based on an acrylic ion selective membrane with a carbon nanotube solid contact layer. For
601   tests in seawater, the sensor was deployed in different coastal marine environments: Arcachon Bay
602   on the Atlantic French coast for 14 hours, Genoa harbor on the Italian Mediterranean coast for 58 and
603   167 hours, and a mix sea-freshwater effluent, the Eyre River, in the Arcachon Bay during high tides
604   for 14 hours. In all these tests the sensor showed good agreement with a reference glass electrode.
605   This was particularly evident during the tests inside the harbour of Genoa where the sensor was
606   compared with that mounted on a commercial multiparametric or Conductivity Temperature Depth
607   (CTD) probe.

608   **5.2 Semiconductor and metal/metal oxide nanomaterials**

609   The most traditional of semiconductor materials, silicon, has found new interesting applications in
610   sensing with the development of Si nanowires (NW). Nanostructures with high packing density and
611   tailored spacing can be fabricated by electron beam lithography on a silicon-on-insulator substrate
612   with high accuracy and reproducibility (Bedner et al., 2013; Park et al., 2010). Choi et al. (2012)
613   produced NWs on boron-doped silicon and deposited a protective layer of Si_3N_4 to ensure better
614   stability. The resistivity of the NW was measured as a function of pH and both short-time noise and
615   long-term drift were measured (Choi et al., 2012). The pH sensitivity of this NW based device has
616   been attributed to charge accumulation at the surface that induces a change in carrier density into the

617 high surface area wires, affecting conductivity. Recently Kim et al. (2014) produced As-doped
618 suspended NWs by a lithographic approach. A linear correlation between normalized conductance
619 and pH was found in the range 4 – 8, with a slope of 0.3 that is twice the slope of non-suspended
620 nanowires (Table 5). The sensitivity was found to exceed the theoretical Nernst limit and, depending
621 on the working current chosen, varied between 87 and 103 mV/pH (Salaün et al., 2014). This
622 unexpected behaviour was observed also in double-gate NW transistors (Ahn et al., 2013) and
623 rationalized taking into account the capacitance of the gates themselves (Knopfmacher et al., 2010).
624 Finally, it is worth reporting a different application of Si NW, grown as a dense array to modify the
625 gate of a FET device. The wires were sputtered with indium-gallium-zinc oxide (IGZO) resulting in a
626 sensitivity of 50 mV/pH (Lin et al., 2013) at a working current of 200 µA.

627 Metal oxide nanostructures can be produced by means of various fabrication techniques, exhibiting
628 interesting electrochemical properties. An example is nanometric sulfated iron oxide (Alizadeh &
629 Jamshidi, 2015). The particles produced by sol-gel were supported with a carbon paste and heat
630 treated at 600°C to produce a regular crystal structure. With an optimized structure, the sensitivity
631 was 57.5 mV/pH and a stability of 1 week was observed, providing the electrode is stored in water or
632 immersed for a few hours in water after storage in dry conditions. Many other semiconducting metal
633 oxides with very interesting properties can be shaped into nanometric wires, ribbons or tubes by
634 different techniques and, interestingly, they can be easily integrated with well established silicon
635 technologies. Titanium and zinc oxide nanotubes/wires are probably the most tested nanomaterials
636 for pH sensing. Both materials show an amphoteric behaviour and can be used in both acidic and
637 alkaline media; the active sites for sensing are oxygen vacancies found at the surface of the oxide
638 structures. Titania nanotubes (NT) with lengths ranging from 33 to 800 nm were produced by
639 anodization of a titanium electrode and embedded in PDMS for testing (Zhao et al., 2010). A nearly
640 Nernstian behaviour was recorded for the nanotube modified electrodes, with best sensitivity and
641 linearity obtained with amorphous titania. Materials prepared in different anodization conditions to
642 produce a dense and thick nanotube layer onto titanium electrodes showed that the production
643 parameters can affect the potentiometric response vs. pH (Albertin et al., 2013). To increase chemical
644 stability, titania can be converted to nitride (TiN), producing a dense array of NTs onto platinum
645 electrodes (Liu et al., 2016). TiN showed a higher pH sensitivity with respect to TiO_2, excellent
646 reproducibility and a good stability over 1 month of storage.

647 Fulati et al. (2009) produced zinc oxide nanotubes and wires, growing them onto gold substrates from
648 a zinc nitrate solution. The response at different pH was measured showing a higher sensitivity for the
649 NTs, explained in terms of higher surface area, and stability of the signal over several days. ZnO
650 nanostructures are increasingly investigated for miniaturized devices (Kumar et al., 2019) and in
651 particular for medical applications (Young & Tang, 2019). A linear response was recorded in the pH
652 range 2 – 12 with aluminium-doped zinc oxide nanosheets (Tsai et al., 2019), tested as the gate layer
653 of an ISFET.

654 A large number of nanostructured oxides have been exploited for pH sensing in different
655 configurations, with a recent trend towards the realization of low cost, flexible devices. High

656 crystallinity tin oxide (SnO_2) nanorods have been produced by a low temperature process onto

657 conductive ITO glass (Li et al., 2012), and this layer was employed as a sensitive gate in an EGFET

658 device. The sensitivity was increased with respect to thin film devices in both the linear and saturation

659 regions of the transistor. Moreover, this device showed low hysteresis and no signal degradation

660 during many hours of operation. Ruthenium oxide nanoparticles, deposited on a plastic supported

661 electrode, have been tested as pH sensitive material in an EGFET configuration (Singh et al., 2019).

662 The device showed a super-Nernstian behaviour, not usually observed for this oxide and a

663 stabilization of the observed drift after 8 hours. Nanostructured platinum electrodes were realized by

664 ink-jet printing onto a plastic substrate by Zea et al. (2019) and modified by electrodeposition of a thin

665 IrO_x amorphous layer. The flexible devices were tested in the pH range 2 – 11 and aged in both dry

666 and wet conditions over 1 year, showing excellent stability.

667 Tungsten oxide (WO_3) is gaining increasing attention as a pH sensitive material. A WO_3 layer was

668 deposited by Zhang and Xu (2009) on a nanostructured electrode composed by aligned CNTs,

669 obtaining a sort of nanopillar. Such modified electrodes showed a sensitivity of about 41 mV/pH, a low

670 drift rate and a good stability after 1 month of storage. Tungsten oxide nanoparticles deposited onto a

671 flexible, plastic supported electrode, showed a linear potential response to pH in the range 5 – 9

672 (Santos et al., 2014). A reduction of the sensitivity was however observed with continuous operation

673 at different pH over ≈ 1h. The same material was deposited onto glassy carbon to realize a sensor for

674 voltammetric measurement of pH (Jamal et al., 2019), obtaining a high sensitivity (60 mV/pH) and

675 linearity of the response. Drift was observed during the initial hours of sensor testing, but the signal

676 stabilized thereafter remaining stable for up to 7 days. Recently, Choi et al. (2019), reported a new

677 type of potentiometric pH sensor based on 1D tungsten oxide nanofibers with an amplified signal

678 exceeding the Nernstian limit. Nanofibers with high porosity were synthesized and stabilized in a

679 chloromethylated triptycene poly (ether sulfone) matrix, allowing a fast proton diffusion into the

680 composite membrane. A high pH sensitivity of -377.5 mV/pH was obtained with the amplified sensor,

681 linearity was acceptable in a narrow pH range (6.9 – 8.9). Testing in artificial seawater demonstrated

682 a negligible effect of dissolved ions.

683 The advantages of nano-scale dimensions can also be exploited, in combination with organic support

684 and/or ion-selective layers, for the realization of multicomponent sensing systems. An ISFET was

685 realized by LbL deposition, using poly(diallyl dimethylammonium) (PDDA) and poly(styrene sulfonate)

686 (PSS) embedding alternate layers of silica and In_2O_3 nanoparticles (Liu & Cui, 2007). The

687 semiconducting indium oxide granted a sufficient conductivity to the device while the protonation/

688 deprotonation of SiO_2 is responsible for pH sensing. A parabolic dependence of current vs. pH was

689 recorded, with higher sensitivity in acid solutions. A development of this concept led to the realization

690 of reliable and sensitive pH sensors based on the LbL assembly of iridium oxide nanoparticles and

691 PDDA. The sensors produced showed a fast response and excellent reproducibility, by using a very

692 low amount of iridium, paving the way for low cost, robust disposable sensors (Jović et al., 2018).

693 Another example of synergistic combination of conducting polymer and nanoparticles was proposed

694 by Kim et al. (2016), who developed a poly(terthiophene benzoic acid) (pTBA) / nanostructured

695 $AuZnO_x$ composite for disposable, solid state pH sensors. These devices were calibrated in the range

696 2 – 12 and showed fast response and stability when tested in biological samples. Lenar et al. (2019)

697 recently proposed RuO_2 nanoparticles showing low resistivity, high stability and redox behaviour, as a

698 solid contact layer between a carbon electrode and a modified PVC-based H^+ selective membrane.

699 The assembly showed a fast, Nernstian response, largely due to the performance of oxide

700 nanoparticles in synergy with the selectivity provided by the polymeric membrane.

Sensing material and setup	Testing range and media	Sensitivity	Stability	Response time	Ref.
Si nanowire + Si_3N_4 passivation layer ISFET	4 – 9 HCl and KOH solutions	5.4%/pH	Maximum drift of 1.68% at pH = 9	n/a	Choi et al., 2012
Si suspended nanowire ISFET	4 – 8 PBS buffer adjusted with HCl and NaOH	0.3/pH (expressed as relative conductance $\Delta G/G_0$)	n/a	n/a	Kim et al., 2014
Polycrystalline Si nanowire ISFET	4 – 9.2	Up to 103 mV/pH	n/a	n/a	Salaün et al., 2014
Si NW Double gated FET	4 – 10 PBS buffer	69 mV/pH	Drift of 27 mV/h	n/a	Ahn et al., 2013
Si NW sputtered with IGZO ISFET	2 – 10	50 mV/pH	n/a	Few seconds	Lin et al., 2013
Si QD EGFET	2 – 12 Commercial buffers	108.3 mV/pH (linearity 98.97%) 2.65 $\mu A^{1/2}$/pH (linearity 99.81%)	Hysteresis of 14 mV cycling pH from 4 to 10.	≈ 100 s	Slewa et al., 2019
Fe_2O_3 nanoparticles Potentiometric	1.5 – 12.5 Negligible influence of common cations	57.5 mV/pH Hysteresis effects ≤ 6%	Stable for > 1 w of storage. Surface can be renewed by rubbing with paper. Reconditioning at pH=7 for few h is needed.	≈ 10 s	Alizadeh & Jamshidi, 2015
TiO_2 nanotubes Potentiometric	2 – 12 Britton-Robinson buffer Negligible interference of common ions (Na^+, K^+, Cl^-, NO_3^-, SO_4^{2-}, F^-, I^-, $Fe(CN)_6^{4-}$)	Up to 59 mV/pH (54 mV/pH before UV irradiation)	n/a		Zhao et al., 2010
TiN nanotubes Potentiometric	2 – 11 Britton-Robinson buffer Low effect of monovalent cations and F^-	55.3 mV/pH	Negligible drift over 200s. Stable after 1 month storage.	4.4 s	Liu et al., 2016
ZnO nanotubes Potentiometric	4 – 12 Commercial buffers Response influenced by $CaCl_2$	45.9 mV/pH	Up to 5 d (tested at day 0, 2 ad 5).		Fulati et al., 2009
Al-doped ZnO ISFET	2 – 12 Commercial buffers	≈ 50 mV/pH	Stable for 12 w at pH 2	0.3 s	Tsai et al., 2019

SnO₂ nanorods EGFET	1 – 13 Commercial buffers	55.2 mV/pH (linear regime) 0.86 μA/pH (saturation regime)	Up to 6h continuous operation	n/a	Li et al., 2012
RuO₂ nanomembrane EGFET	2 – 12 Commercial buffers Low interference of mono and divalent cations	65.1 mV/pH (linear regime) 1.05 μA/pH (saturation regime)	Drift of 2 mV/h, stabilizes after 8 h of immersion	n/a	Singh et al., 2019
IrOₓ onto nanostructured Pt Potentiometric	2 – 11 KCl solution adjusted with strong acid/base	70.9 mV/pH Standard deviation < 1%.	Stable for 1 year, dry or immersed in PBS. Sensitivity stabilizes after 1 month.	6 – 8 s	Zea et al., 2019
WO₃ layer on CNTs Potentiometric	2 – 12 Britton-Robinson buffer	40.73 mV/pH	Standard error <1% Stable after 1 month of storage	30 s (pH 4) 90 s (pH 12	Zhang & Xu, 2009
WO₃ nanoparticles Potentiometric	5 – 9 Commercial buffers	56.7 ± 1.3 mV/pH	Sensitivity reduction over time	28 s	Santos et al., 2014
WO₃ nanoparticles Voltammetry	3 – 11 Phosphate buffer Tested in vinegar	60.0 ± 0.01 mV/pH	Average drift of 33 mV over 3 h. 95% sensitivity retained after 7 d of use.	n/a	Jamal et al., 2019
WO₃ nanofibers Potentiometric, amplified	3 – 11 Commercial buffers **Tested in artificial seawater (pH 8.0 – 7.6)**	38.9 mV/pH (amplified to 377.5 mV/pH)	n/a	n/a	Choi et al., 2019
IrOx / PDDA Potentiometric	3 – 10 Commercial buffers	59 mV/pH	n/a	3 s	Jović et al., 2018
pTBA / AuZnOx Potentiometric	2 – 13 Commercial buffers Also tested in saliva and urine samples	59.2 ± 0.5 mV/pH	Stable for cyclic measurements (200 s). Good stability upon storage for 15 d	1 s	Kim et al., 2016
RuO₂ np solid contact + PVC based membrane Potentiometric	2 – 12 Tris buffer Good selectivity against monovalent cations	59 mV/pH	Stable for 1 w of daily calibrations	n/a	Lenar et al., 2019

Table 5. pH sensors based on semiconductor and metal/metal oxide nanomaterials. In bold, sensors that have been tested in seawater.

None of the potentiometric pH sensors listed in Table 5 was tested in seawater apart from the WO₃ nanofibers potentiometric amplified sensor realized by Choi et al. (2019). They tested such sensors in artificial seawater and calibrated the reading against a commercial pH meter, Due to the high sensitivity obtained through the amplification, the authors concluded that their new pH sensor is promising for portable and low-cost applications for the monitoring of seawater; however, stability and long term performances were not assessed.

6. Conclusions

711

pH is a key parameter in many chemical, biological and biogeochemical phenomena and is of particular interest in environmental monitoring. Ion sensitive glass electrodes are the most used sensors for pH measurements, but new solutions for the realization of robust, precise and affordable pH sensors are actively investigated.

In this review, we have presented the most recent developments in pH sensing materials, reporting sensor performances and main parameters. Solid state sensors based on inorganic materials, (metals of semiconductors), and carbon based materials (polymers and carbon particles) have been reviewed, revealing a general trend towards the realization of miniaturized, low cost/disposable sensors.

The development of nano-engineered materials and composites as active sensing elements has emerged as a promising strategy to improve sensitivity, response time, flexibility and ease of fabrication. Thin films and nanomaterials based on metal oxides provide good sensing performances and relatively good stability and can be easily integrated in potentiometric sensors or silicon-based FET devices. Examples of application of metal oxide pH sensors in different environments, including seawater, have been reported pointing out their robustness and flexibility.

Carbon nanoparticles, despite having attracted a large research effort, are not so stable in their response (sensitive to surface defects, functional groups and morphology), nor easy to produce and handle. Polymer-based sensors, finally, seems to be non-competitive in terms of precision and stability. However, the limitations shown by this class of materials can be overcome by properly combining them. In this respect, the synergy observed between polymeric components, and inorganic nanomaterials seems to be a key factor for the realization of robust and affordable sensors. Polymers can be used as efficient ion-selective or protective elements, to enhance the response of inorganic sensing elements and decrease the interference of dissolved ions. On the other hand, the response and the stability of pH sensitive polymers can be greatly improved by combining them with conductive and semiconductive nanomaterials, as shown for the most common electroactive polymer, PANI, and for polydopamine.

For each sensor class, results of testing in seawater, when available, have been reported and discussed. Only few new sensors have been designed for seawater, however, the examples reported show promising results, in terms of sensitivity, selectivity vs. interfering ions and stability. While some inorganic material (metal oxides) has shown good sensing performances at sea, among the devices based on polymers or carbon nanomaterials the only ones successfully tested in seawater are based on composite or multilayer structures. Design refinement and extensive field testing and validation are needed to assess the suitability of the sensors presented for seawater monitoring. Even if the possibility to replace well-established measurement technologies like glass electrodes and spectrophotometry looks, as yet, unrealistic, in the near future, robust, miniaturized, integrated arrays of solid state electrochemical pH sensors can represent a valuable alternative for specific applications.

749

753 **References**

754 Adhikari, B., & Majumdar, S. (2004). Polymers in sensor applications. *Progress in Polymer Science,*
755   29(7), 699–766. doi: 10.1016/j.progpolymsci.2004.03.002

756 Ahn, J.-H., Kim, J.-Y., Seol, M.-L., Baek, D.J., Guo, Z., Kim, C.-H., Choi, S.-J., & Choi, Y.-K. (2013). A
757   pH sensor with a double-gate silicon nanowire field-effect transistor. *Applied Physics Letters,* 102,
758   083701. doi: 10.1063/1.4793655

759 Albertin, K.F., Carreño, M.N.P., & Pereyra, I. (2013). Study of TiO_2 Nanotubes for Sensors and
760   Integrated Devices. *Precision Instrument and Mechanology*, 2(3), 114-121.

761 Alizadeh, T., & Jamshidi, F. (2015). Synthesis of nanosized sulfate-modified α-Fe_2O_3 and its use for
762   the fabrication of all-solid-state carbon paste pH sensor. *Journal of Solid State Electrochemistry,*
763   19, 1053–1062. doi: 10.1007/s10008-014-2716-4

764 Ameri, S.K., Singh, P.K., & Sonkusale, S.R. (2016). Three dimensional graphene transistor for ultra-
765   sensitive pH sensing directly in biological media. *Analytica Chimica Acta*, 934, 212-217. doi:
766   10.1016/j.aca.2016.05.048

767 Amiri, M., Amali, E., Nematollahzadeh, A., & Salehniya, H. (2016). Poly-dopamine films: Voltammetric
768   sensor for pH monitoring. *Sensors and Actuators B: Chemical*, 228, 53–58. doi:
769   10.1016/j.snb.2016.01.012

770 Ang, P.K., Chen, W., Wee, A.T.S. & Ping, K. (2008). Solution-Gated Epitaxial Graphene as pH
771   Sensor. *Journal of the American Chemical Society,* 130, 14392–14393. doi: 10.1021/ja805090z

772 Ates, M. (2013). A review study of (bio)sensor systems based on conducting polymers. *Materials*
773   *Science and Engineering C*, 33(4), 1853–1859. doi: 10.1016/j.msec.2013.01.035

774 Athavale, R., Dinkel, C., Wehrli, B., Bakker, E., Crespo, G.A., & Brand, A. (2017). Robust solid-
775   contact ion selective electrodes for high-resolution in situ measurements in fresh water systems.
776   *Environmental Science and Technology Letters*, 4(7), 286-291. doi: 10.1021/acs.estlett.7b00130

777 Back, J.H., & Shim, M. (2006). pH-Dependent Electron-Transport Properties of Carbon Nanotubes.
778   *Journal of Physical Chemistry B*, 110, 23736-23741. doi: 10.1021/jp063260x

779 Bangar, M., Chen, W., Myung, N., & Mulchandani, A. (2010). Conducting polymer 1-dimensional
780   nanostructures for FET sensors. *Thin Solid Films*, 519, 964-973. doi: 10.1016/j.tsf.2010.08.023

781 Banna, M.H., Najjaran, H., Sadiq, R., Imran, S.A., Rodriguez, M.J., & Hoorfar, M. (2014). Miniaturized
782   water quality monitoring pH and conductivity sensors. *Sensors and Actuators B: Chemical*, 193,
783   434-441. doi: 10.1016/j.snb.2013.12.002

784 Bao, Q., Yang, Z., Song, Y., Fan, M., Pan, P., Liu, J., Liao, Z., & Wei, J. (2019). Printed flexible
785   bifunctional electrochemical urea-pH sensor based on multiwalled carbon nanotube/polyaniline
786   electronic ink. *Journal of Materials Science: Materials in Electronics*, 30(2), 1751-1759. doi:
787   10.1007/s10854-018-0447-5

788 Barton, J., Begoña González García, M., Hernández Santos, D., Fanjul-Bolado, P., Ribotti, A.,
789   McCaul, M., Diamond, D., & Magni P. (2016). Screen-printed electrodes for environmental
790   monitoring of heavy metal ions: a review. *Microchimica Acta*, 183, 503-517. doi: 10.1007/s00604-
791   015-1651-0

792 Bedner, K., Guzenko, V.A., Tarasov, A., Wipf, M., Stoop, R.L., Just, D., Rigante, S., Fu, W.,
793   Minamisawa, R.A., David, C., & Calame, M. (2013). pH response of silicon nanowire sensors:
794   impact of nanowire width and gate oxide. *Sensors and Materials*, 25(8), 567-576. doi:
795   10.18494/SAM.2013.890

796 Bergveld, P. (2003). Thirty years of ISFETOLOGY: What happened in the past 30 years and what
797   may happen in the next 30 years. *Sensors and Actuators B: Chemical*, 88(1), 1–20. doi:
798   10.1016/S0925-4005(02)00301-5

799 Boeva, Z.A., Milakin, K.A., Pesonen, M., Ozerin, A.N., Sergeyev, V.G., & Lindfors, t. (2014).
800   Dispersible composites of exfoliated graphite and polyaniline with improved electrochemical
801   behaviour for solid-state chemical sensor applications. *RSC Advances*, 4, 46340. doi:
802   10.1039/c4ra08362h

803 Brooke, M., Cole, E., Dale, J., Prasad, A., Quach, H., Bau, B., Nowacek, D., & Bhatt, E. (2016). An
804   ocean sensor for measuring the seawater electrochemical response of 8 metals referenced to zinc,
805   for determining ocean pH. *9th International Conference on Sensing Technology (ICST)*, Auckland
806   (NZ), 8-11 December 2015, 147-150. doi: 10.1109/ICSensT.2015.7438381

807 Buck, R.P., Rondinini, S., Covington, A.K., Baucke, F.G.K., Brett, C.M.A., Camões, M.F., Milton,
808   M.J.T., Mussini, T., Naumann, R., Pratt, K.W., & Spitzer, P. (2002). Measurement of pH. Definition,
809   standards, and procedures. *Pure Appl. Chem.,* 74(11), 2169–2200. http://hdl.handle.net/1808/8412

810 Bushinsky, S.M., Takeshita, Y., & Williams, N.L. (2019). Observing Changes in Ocean Carbonate
811   Chemistry: Our Autonomous Future. *Current Climate Change Reports*, 5(3), 207-220. doi:
812   10.1007/s40641-019-00129-8

813 Byrne, R.H. (2014). Measuring Ocean Acidification: New Technology for a New Era of Ocean
814   Chemistry. *Environmental Science and Technology*, 48(10), 5352-5360. doi: 10.1021/es405819p

815 Cachet-Vivier, C., Tribollet, B., Vivier, V. (2010). Cavity microelectrode for studying manganese
816   dioxide powder as pH sensor. *Talanta*, 82(2), 555–559. doi: 10.1016/j.talanta.2010.05.006

817 Chen, X.M., Wu, G.H., Jiang, Y.Q., Wang, Y.R., & Chen, X. (2011). Graphene and graphene-based
818   nanomaterials: the promising materials for bright future of electroanalytical chemistry. *Analyst*,
819   136(22), 4631-40. doi: 10.1039/c1an15661f

820 Cheng, Z., Li, Q., Li, Z., Zhou, Q., & Fang, Y. (2010). Suspended Graphene Sensors with Improved
821   Signal and Reduced Noise. *Nano Letters*, 10, 1864–1868. doi: 10.1021/nl100633g

822   Chien, Y.-S., Tsai, W.-L., Lee, I-C., Chou, J.-C., & Cheng. H.-C. (2012). Novel Ph Sensor Of Egfets
823   With Laser-Irradiated Carbon-Nanotube Network. *IEEE Electron Device Letters*, 33(11), 1622-
824   1624. doi: 10.1109/LED.2012.2213794

825   Chinnathambi, S., & Euverink. G.J.W. (2018). Polyaniline functionalized electrochemically reduced
826   graphene oxide chemiresistive sensor to monitor the pH in real time during microbial
827   fermentations. *Sensors and Actuators B: Chemical*, 264, 38–44. doi: 10.1016/j.snb.2018.02.087

828   Choi, J.-S, Savagatrup, S., Kim, Y., Lang, J.H., & Swager, T.M. (2019). Precision pH sensor based on
829   WO_3 nanofiber-polymer composites and different amplification. *ACS Sensors*, 4(10), 2593-2598.
830   doi:10.1021/acssensors.9b01579

831   Choi, S., Park, I., Hao, Z., Holman, H.-Y. N., & Pisano, A.P. (2012). Quantitative studies of long-term
832   stable, top-down fabricated silicon nanowire pH sensors. *Applied Physics A*, 107, 421–428. doi:
833   10.1007/s00339-011-6754-9

834   Cisternas, R., Kahlert, H., Scholz, F., & Wulff, H. (2015). Direct contact tungsten bronze electrodes for
835   calibration-free potentiometric pH measurements. *Electrochemistry Communications*, 60, 17-20.
836   doi: 10.1016/j.elecom.2015.07.017

837   Cisternas, R., Ballesteros, L., Valenzuela, M.L., Kahlert, H., & Scholz, F. (2017). Decreasing the time
838   response of calibration-free pH sensors based on tungsten bronze nanocrystals. *Journal of
839   Electroanalytical Chemistry*, 801, 315–318. doi: 10.1016/j.jelechem.2017.08.005

840   Clarke, J.S., Achterberg, E.P., Rérolle, V.M.C., Abi Kaed Bey, S., Floquet, C.F.A., Mowlem, M.C.
841   (2015). Characterisation and deployment of an immobilised pH sensor spot towards surface ocean
842   pH measurements. *Analytica Chimica Acta*, 897, 69–80. doi: 10.1016/j.aca.2015.09.026

843   Cleary, J., McCaul, M., Diamond, D., García, M.B.G., Díez, C., Rovira, C., Challiss, M., Lassoued, Y.,
844   Ribotti, A., Sáez, J. (2014). COMMON SENSE: Cost-effective sensors, interoperable with
845   international existing ocean observing systems, to meet EU policies requirements. *2014 IEEE
846   Sensor Systems for a Changing Ocean (SSCO 2014)*, 1-7, doi: 10.1109/SSCO.2014.7000384

847   Crespo, G.A., Gugsa, D., Macho, S., & Rius, F.X. (2009). Solid-contact pH-selective electrode using
848   multi-walled carbon nanotubes. *Analytical and Bioanalytical Chemistry*, 395, 2371-2376. doi:
849   10.1007/s00216-009-3127-8

850   Cuartero, M., Pankratova, N., Cherubini, T., Crespo, G., Massa, F., Confalonieri, F., & Bakker, E.
851   (2017). In Situ Detection of Species Relevant to the Carbon Cycle in Seawater with Submersible
852   Potentiometric Probes. *Environmental Science & Technology Letters*, 4. doi:
853   10.1021/acs.estlett.7b00388

854   Culebras, M., Gómez, C.M., & Cantarero, A. (2014). Review on Polymers for Thermoelectric
855   Applications. *Materials*, 7(9), 6701-6732. doi: 10.3390/ma7096701

856   Cullison Gray, S.E., DeGrandpre, M.D., Moore, T.S., Martz, T.R., Friederich, G.E., & Johnson, K.S.
857   (2011). Applications of in situ pH measurements for inorganic carbon calculations. *Marine*
858   *Chemistry*, 125(1-4), 82–90. doi: 10.1016/j.marchem.2011.02.005

859   Dai, C., Chan, C.-W.I., Barrow, W., Smith, A., Song, P., Potier, F., Wadhawan, J.D., Fisher, A.C., &
860   Lawrence, N.S. (2016). A Route to Unbuffered pH Monitoring: A Novel Electrochemical Approach.
861   *Electrochimica Acta*, 190, 879-886. doi: 10.1016/j.electacta.2016.01.004

862   Fu, W., Nef, C., Knopfmacher, O., Tarasov, A., Weiss, M., Calame, M., & Schönenberger, C. (2011).
863   Graphene Transistors Are Insensitive to pH Changes in Solution. *Nano Letters*, 11(9), 3597–3600.
864   doi: 10.1021/nl201332c

865   Fulati, A., Usman Ali, S.M., Riaz, M., Amin, G., Nur, O., & Willander, M. (2009). Miniaturized pH
866   Sensors Based on Zinc Oxide Nanotubes/Nanorods. *Sensors*, 9(11), 8911-8923. doi:
867   10.3390/s91108911

868   Gao, W., & Song, J. (2009). Polyaniline Film Based Amperometric pH Sensor Using A Novel
869   Electrochemical Measurement System. *Electroanalysis*, 21(8), 973-978. doi:
870   10.1002/elan.200804500

871   Gill, E., Arshak, A., Arshak, K.,& Korostynska, O. (2008). Conductometric pH sensor based on novel
872   conducting polymer composite thick films. *Proceedings of the 2008 31st International Spring*
873   *Seminar on Electronics Technology*, 478–483. doi: 10.1109/ISSE.2008.5276613

874   Glab, S., Hulanicki, A., Edwall, G., & Ingman F. (1989). Metal-Metal Oxide and Metal Oxide
875   Electrodes as pH Sensors. *Critical Reviews in Analytical Chemistry*, 21(1), 29-47. doi:
876   10.1080/10408348908048815

877   González Durán, E., Cuaya, M.P., Gutiérrez, M.V. & Ancona León, J. (2018). Effects of Temperature
878   and pH on the Oxidative Stress of Benthic Marine Invertebrates. *Biology Bullettin,* 45, 610–616.
879   https://doi.org/10.1134/S1062359018660019

880   Gou, P., Kraut, N.D., Feigel, I.M., Bai, H., Morgan, G.J., Chen, Y., Tang, Y., Bocan, K., Stachel, J.,
881   Berger, L., Mickle, M., Sejdic, E., & Star, A., (2014). Carbon Nanotube Chemiresistor for Wireless
882   pH Sensing. *Scientific Reports*, 4, 4468. doi: 10.1038/srep04468

883   Grozdanov, A., Petrovski, A., Paunovic, P., Dimitrov, T.A., & Avella M. (2018). MWCNT/Polyaniline
884   nanocomposites used for pH nanosensors of marine waters. In M. Cocca, E. Di Pace, M. Errico,
885   G. Gentile, A. Montarsolo, R. Mossotti (Eds.), *Proceedings of the International Conference on*
886   *Microplastic Pollution in the Mediterranean Sea*, (pp. 231-238). Springer International Publishing.
887   doi: 10.1007/978-3-319-71279-6_32

888   Grozdanov, A., Petrovski, A., Avella, M., Paunovic, P., Errico, E.M., Avolio, R., Gentile, G., De Falco,
889   F., & Dimitrov, T. A. (2019). Spectroscopic study of nanocomposite based on PANI and Carbon
890   nanostructures for pH sensors. *Bulgarian Chemical Communications*, 51(D), 36-41.

891 Gupta, N., Sharma, S., Mir, I.A., & Kumar, D. (2006). Advances in sensors based on conducting

892   polymers. *Journal of Scientific and Industrial Research*, 65(7), 549-557.

893   http://nopr.niscair.res.in/handle/123456789/4862

894 Hayat, A., & Marty, J.L. (2014). Disposable screen printed electrochemical sensors: tools for

895   environmental monitoring. *Sensors*, 14(6), 10432-53. doi: 10.3390/s140610432

896 Heller, I., Chatoor, S., Mannik, J., Zevenbergen, M.A.G., Dekker, C., & Lemay, S.G. (2010). Influence

897   of Electrolyte Composition on Liquid-Gated Carbon Nanotube and Graphene Transistors. *Journal

898   of the American Chemical Society*, 132(48), 17149-17156. doi: 10.1021/ja104850n

899 Hu, J., Ho, K.T., Zou, X.U., Smyrl, W.H., Stein, A., & Bühlmann, P. (2015). All-Solid-State Reference

900   Electrodes Based on Colloid-Imprinted Mesoporous Carbon and their Application in Disposable

901   Paper-based Potentiometric Sensing Devices. *Analytical Chemistry*, 87(5), 2981–2987. doi:

902   10.1021/ac504556s

903 Huang, W.S., Humphrey, B.D., & MacDiarmid, A.G. (1986). Polyaniline, a novel conducting polymer.

904   Morphology and chemistry of its oxidation and reduction in aqueous electrolytes. *J. Chem. Soc.,

905   Faraday Trans. 1: Physical Chemistry in Condensed Phases*, 82(8), 2385-2400. doi:

906   10.1039/F19868202385

907 Jamal, M., Razeeb, K.M., Shao, H., Islam, J., Akhter, I., Furukawa, H., & Khosla, A. (2019).

908   Development of Tungsten Oxide Nanoparticle Modified Carbon Fibre Cloth as Flexible pH Sensor.

909   *Scientific Reports*, 9(1), Article number 4659. doi: 10.1038/s41598-019-41331-w

910 Jang, H., & Lee, J. (2020). Iridium oxide fabrication and application: A review. *Journal of Energy

911   Chemistry*, 46, 152-172. doi: 10.1016/j.jechem.2019.10.026

912 Jin, Q. & Kirk, M.F. (2018). pH as a Primary Control in Environmental Microbiology: 1.

913   Thermodynamic Perspective. *Frontiers in Environmental Science,* 6:21. doi:

914   10.3389/fenvs.2018.00021

915 Johnson, K.S., Jannasch, H.W., Coletti, L.J., Elrod, V.A., Martz, T.R., Takeshita, Y., Carlson, R.J., &

916   Connery, J.C. (2016). Deep-Sea DuraFET: A Pressure Tolerant pH Sensor Designed for Global

917   Sensor Networks. *Analytical Chemistry*, 88(6), 3249-3256. doi: 10.1021/acs.analchem.5b04653

918 Jović, M., Hidalgo-Acosta, J.C., Lesch, A., Costa Bassetto, V., Smirnov, E., Cortés-Salazar, F., &

919   Girault, H.H. (2018). Large-scale layer-by-layer inkjet printing of flexible iridium-oxide based pH

920   Sensors. *Journal of Electroanalytical Chemistry*, 819, 384–390. doi:

921   10.1016/j.jelechem.2017.11.032

922 Jung, M.W., Myung, S., Song, W., Kang, M.A., Kim, S.H., Yang, C.S., Lee, S.S., Lim, J., Park, C.Y.,

923   Lee, J.O., & An, K.S. (2014). Novel fabrication of flexible graphene-based chemical sensors with

924   heaters using soft lithographic patterning method. *ACS Applied Materials & Interfaces*, 6(16),

925   13319-13323. doi: 10.1021/am502281t

926   Khan, M.I., Mukherjee, K., Shoukat, R. & Dong, H. (2017). A review on pH sensitive materials for
927   sensors and detection methods. *Microsystem Technologies*, 23, 4391–4404. doi: 10.1007/s00542-
928   017-3495-5

929   Kim, D.-M., Cho, S.J., Cho, C.-H., Kim, K.B., Kim, M.-Y., & Shim, Y.-B. (2016). Disposable all-solid-
930   state pH and glucose sensors based on conductive Polymer covered hierarchical AuZn oxide.
931   *Biosensors and Bioelectronics*, 79, 165–172. doi: 10.1016/j.bios.2015.12.002

932   Kim, K., Park, C., Rim, T., Meyyappan, M., & Lee, J.-S. (2014). Electrical and pH Sensing
933   Characteristics of Si Nanowire-Based Suspended FET Biosensors. *Proceedings of the 14th IEEE*
934   *International Conference on Nanotechnology Toronto*, Canada, August 18-21

935   Kim, T.Y., & Yang, S. (2014). Fabrication method and characterization of electrodeposited and heat-
936   treated iridium oxide films for pH sensing. *Sensors and Actuators B: Chemical*, 196, 31-38. doi:
937   10.1016/j.snb.2014.02.004

938   King, D.W., & Kester, D.R. (1989). Determination of seawater pH from 1.5 to 8.5 using colorimetric
939   indicator. *Marine Chemistry*, 26(1), 5-20. doi: 10.1016/0304-4203(89)90061-3

940   Kinoshita, E., Ingman, F., Edwalla, G., Thulina, S., & Głąb, S. (1986). Polycrystalline and
941   monocrystalline antimony, iridium and palladium as electrode material for pH-sensing electrodes.
942   *Talanta*, 33(2), 125-134. doi: 10.1016/0039-9140(86)80028-5

943   Knopfmacher, O., Tarasov, A., Fu, W., Wipf, M., Niesen, B., Calame, M., & Schönenberger, C. (2010).
944   Nernst Limit in Dual-Gated Si-Nanowire FET Sensors. *Nano Letters*, 10(6), 2268–2274. doi:
945   10.1021/nl100892y

946   Koncki, R., & Mascini, M. (1997). Screen-printed ruthenium dioxide electrodes for pH measurements.
947   *Analytica Chimica Acta*, 351(1–3), 143–149. doi: 10.1016/S0003-2670(97)00367-X

948   Korostynska, O., Arshak, K., Gill, E., & Arshak, A. (2007). Review on state-of-the-art in Polymer
949   Based pH sensors. *Sensors*, 7(12), 3027-3042. doi: 10.3390/s7123027

950   Kroeker, K.J., Kordas, R., Crim, R., Hendriks, I.E., Ramajo, L., Singh, G.S., Duarte, C.D., & Gattuso,
951   J.-P. (2013). Impacts of ocean acidification on marine organisms: quantifying sensitivities and
952   interaction with warming. *Global Change Biology*, 19(6), 1884-1896. doi: 10.1111/gcb.12179

953   Kumar, A., Kumar, N., Aniley, A.A., Fernandez, R.E., & Bhansali, S. (2019). Hydrothermal growth of
954   zinc oxide (ZnO) nanorods (NRs) on screen printed IDEs for ph measurement application. *Journal*
955   *of the Electrochemical Society*, 166, B3264-B3270. doi: 10.1149/2.0431909jes

956   Kumar, N., Sutradhar, M., Kumar, J., & Panda, S. (2017). Role of deposition and annealing of the top
957   gate dielectric in a-IGZO TFT-based dual-gate ion-sensitive field-effect transistors. *Semiconductor*
958   *Science and Technology*, 32, 035013. doi: 10.1088/1361-6641/aa5584

959   Kuo, L.-M., Chou, Y.-C., Chen, K.-N., Lu, C.-C., Chao, S. (2014). A precise pH microsensor using RF-
960   sputtering IrO_2 and Ta_2O_5 films on Pt-electrode. *Sensors and Actuators B: Chemical*, 193, 687-
961   691. doi: 10.1016/j.snb.2013.11.109

962 Lacoue-Labarthe, T., Nunes, P.A.L.D., Ziveri, P., Cinar, M., Gazeau, F., Hilmi, N., Moschella, P., Safa,
963   A., Sauzade, D., & Turley, C. (2016). Impacts of ocean acidification in a warming Mediterranean
964   Sea: An overview. *Regional Studies in Marine Science*, 5, 1-11. doi: 10.1016/j.rsma.2015.12.005

965 Lai, C.-Z., DeGrandpre, M.D., & Darlington, R.C. (2018). Autonomous Optofluidic Chemical Analyzers
966   for Marine Applications: Insights from the Submersible Autonomous Moored Instruments (SAMI)
967   for pH and pCO_2. *Frontiers in Marine Science*, 4, 438. doi: 10.3389/fmars.2017.00438

968 Lakard, B., Segut, O., Lakard, S., Herlem, G., & Gharbi, T. (2007). Potentiometric miniaturized pH
969   sensors based on polypyrrole films. *Sensors and Actuators B: Chemical*, 122, 101-108. doi:
970   10.1016/j.snb.2006.04.112

971 Lee, D., & Cui, T. (2010). Low-cost, transparent, and flexible single-walled carbon nanotube
972   nanocomposite based ion-sensitive field-effect transistors for pH/glucose sensing. *Biosensors and
973   Bioelectronics*, 25(10), 2259–2264. doi: 10.1016/j.bios.2010.03.003

974 Lei, K.F., Lee, K.-F., & Yang, S.-I (2012). Fabrication of carbon nanotube-based pH sensor for paper-
975   based microfluidics. *Microelectronic Engineering*, 100, 1–5. doi: 10.1016/j.mee.2012.07.113

976 Lenar, N., Paczosa-Bator, B., & Piech, R. (2019). Ruthenium dioxide nanoparticles as a high-capacity
977   transducer in solid-contact polymer membrane-based pH-selective electrodes. *Microchimica Acta*,
978   186(12), Article n. 777. doi: 10.1007/s00604-019-3830-x

979 Li, H.-H., Dai, W.-S., Chou, J.-C., & Cheng, H.-C. (2012). An Extended-Gate Field-Effect Transistor
980   With Low-Temperature Hydrothermally Synthesized SnO_2 Nanorods as pH Sensor. *IEEE Electron
981   Device Letters*, 33(10), 1495-1497. doi: 10.1109/LED.2012.2210274

982 Li, Q., Li, H., Zhang, J., & Xu, Z. (2011). A novel pH potentiometric sensor based on electrochemically
983   synthesized polybisphenol A films at an ITO electrode. *Sensors and Actuators B: Chemical*, 155,
984   730–736. doi: 10.1016/j.snb.2011.01.038

985 Li, X., Cai, W., An, J., Kim, S., Nah, J., Yang, D., Piner, R., Velamakanni, A., Jung, I., Tutuc, E.,
986   Banerjee, S.K., Colombo, L., & Ruoff, R.S. (2009). Large-area synthesis of high-quality and
987   uniform graphene films on copper foils. *Science*, 324(5932), 1312-1314. doi:
988   10.1126/science.1171245

989 Li, Y., Mao, Y., Xiao, C., Xu, X., & Li, X. (2020). Flexible pH sensor based on a conductive PANI
990   membrane for pH monitoring. *RSC Advances*, 10, 21-28. doi: 10.1039/C9RA09188B

991 Lin, J.-C., Huang, B.-R., & Yang, Y.-K. (2013). IGZO nanoparticle-modified silicon nanowires as
992   extended-gate field-effect transistor pH sensors. *Sensors and Actuators B: Chemical*, 184, 27–32.
993   doi: 10.1016/j.snb.2013.04.060

994 Liu, M., Ma, Y., Su, L., Chou, K.-C., & Hou, X. (2016). A titanium nitride nanotube array for
995   potentiometric sensing of pH. *Analyst*, 141(5), 1693-1699. doi: 10.1039/c5an02675j

996   Liu, Y., & Cui, T. (2007). Ion-sensitive field-effect transistor based pH sensors using nano self-
997   assembled polyelectrolyte/nanoparticle multilayer films. *Sensors and Actuators B: Chemical*, 123,
998   148–152. doi:10.1016/j.snb.2006.08.006

999   Loh, K.J., Lynch, J.P., & Kotov, N.A. (2007). Passive wireless strain and pH sensing using carbon
1000   nanotube-gold nanocomposite thin films. In M. Tomizuka, C.-B. Yun, V. Giurgiutiu (Eds.), Sensors
1001   and Smart Structures Technologies for Civil, Mechanical, and Aerospace Systems, *Processing of*
1002   *SPIE*, 6529, 652919-652931. doi: 10.1117/12.715826

1003   Lonsdale, W., Wajrak, M., & Alameh, K. (2018). Manufacture and application of RuO_2 solid-state
1004   metal-oxide pH sensor to common beverages. *Talanta*, 180, 277-281. doi:
1005   10.1016/j.talanta.2017.12.070

1006   Mailly-Giacchetti, B., Hsu, A., Wang, H., Vinciguerra, V., Pappalardo, F., Occhipinti, L., Guidetti, E.,
1007   Coffa, S., Kong, J., & Palacios, T. (2013). pH sensing properties of graphene solution-gated field-
1008   effect transistors. *Journal of Applied Physics*, 114, 084505. doi: 10.1063/1.4819219

1009   Manjakkal, L., Cvejin, K., Kulawik, J., Zaraska, K., Szwagierczak, D., & Socha, R.P. (2014).
1010   Fabrication of thick film sensitive RuO_2-TiO_2 and Ag/AgCl/KCl reference electrodes and their
1011   application for pH measurements. *Sensors and Actuators B: Chemical*, 204, 57–67.
1012   doi:10.1016/j.snb.2014.07.067

1013   Manjakkal, L., Synkiewicz, B., Zaraska, K., Cvejin, K., Kulawik, J., & Szwagierczak, D. (2016).
1014   Development and characterization of miniaturized LTCC pH sensors with RuO_2 based sensing
1015   electrodes. *Sensors and Actuators B: Chemical*, 223, 641–649. doi: 10.1016/j.snb.2015.09.135

1016   Marion, G. M., Millero, F. Camões, M.F., Spitzer, P., Feistel, R., & Chen, C.T.A. (2011). pH of
1017   seawater. *Marine Chemistry*, 126, 89-96. doi: 10.1016/j.marchem.2011.04.002

1018   Martin, A., &. Escarpa, A. (2014). Graphene: The cutting–edge interaction between chemistry and
1019   electrochemistry. *TrAC Trends in Analytical Chemistry,* 56, 13-26. doi: 10.1016/j.trac.2013.12.008

1020   Martz, T., McLaughlin, K., Weisberg, S.B. (2015). Best Practices for autonomous measurement of
1021   seawater pH with the Honeywell Durafet pH sensor. *Technical Report 861. California Current*
1022   *Acidification Network. Santa Barbara, CA.*
1023   *http://ftp.sccwrp.org/pub/download/DOCUMENTS/TechnicalReports/861_CCAN_Durafet_Best_Pr*
1024   *actices_Manual.pdf*

1025   McLaughlin, K., Dickson, A., Weisberg, S.B., Coale, K., Elrod, V., Hunter, C., Johnson, K.S., Kram, S.,
1026   Kudela, R., Martz, T., Negrey, K., Passow, U., Shaughnessy, F., Smith, J.E., Tadesse, D.,
1027   Washburn, L., & Weis, K.R. (2017a). An evaluation of ISFET sensors for coastal pH monitoring
1028   applications. *Regional Studies in Marine Science*, 12, 11-18. doi: 10.1016/j.rsma.2017.02.008

1029   McLaughlin, K., Nezlin, N.P., Weisberg, S.B., Dickson, A.G., Booth, J.A., Cash, C.L., Feit, A., Gully,
1030   J.R., Johnson, S., Latker, A., Mengel, M.J., Robertson, G.L., Steele, A., & Terriquez, L. (2017b).
1031   An evaluation of potentiometric pH sensors in coastal monitoring applications. *Limnology and*
1032   *Oceanography: Methods*, 15, 679-689. doi: 10.1002/lom3.10191

1033 Michalska, A. (2012). All-Solid-State Ion Selective and All-Solid-State Reference Electrodes.
1034   *Electroanalysis*, 24, 1253–1265. doi: 10.1002/elan.201200059

1035 Millero, F.J., DiTrolio, B., Suarez, A.F., & Lando, G. (2009). Spectroscopic measurements of the pH in
1036   NaCl brines. *Geochimica Cosmochimica Acta*, 73, 3109–3114. doi: 10.1016/j.gca.2009.01.037

1037 Moya, A., Pol, R., Martínez-Cuadrado, A., Villa, R., Gabriel, G., & Baeza, M. (2019). Stable Full-Inkjet-
1038   Printed Solid-State Ag/AgCl Reference Electrode. *Analytical Chemistry*, 91(24), 15539-15546. doi:
1039   10.1021/acs.analchem.9b03441

1040 Newton, J.A., Feeley, R.A., Jewett, E.B., Williamson, P., & Mathis, J. (2015). *Global Ocean*
1041   *Acidification Observing Network: Requirements and Governance Plan (2nd edition).* GOA-ON.
1042   http://www.goa-on.org/documents/general/GOA-ON_2nd_edition_final.pdf

1043 Novoselov, K.S., Falko, V.I., Colombo, L., Gellert, P.R., Schwab, M.G., & Kim, K. (2012). A roadmap
1044   for graphene. *Nature*, 490(7419), 192-200. doi: 10.1038/nature11458

1045 Ohno, Y., Maehashi, K., Yamashiro, Y., & Matsumoto, K. (2009). Electrolyte-Gated Graphene Field-
1046   Effect Transistors for Detecting pH and Protein Adsorption. *Nano Letters*, 9(9), 3318-3322. doi:
1047   10.1021/nl901596m

1048 Ohno, Y., Maehashi, K., & Matsumoto, K. (2010). Chemical and biological sensing applications based
1049   on graphene field-effect transistors. *Biosensors and Bioelectronics*, 26, 1727–1730. doi:
1050   10.1016/j.bios.2010.08.001

1051 Okazaki, R.R., Sutton, A.J., Feely, R.A., Dickson, A.G., Alin, S.R., Sabine, C.L., Bunje, P.M.E., &
1052   Virmani, J.I. (2017). Evaluation of marine pH sensors under controlled and natural conditions for
1053   the Wendy Schmidt Ocean Health XPRIZE. *Limnology and Oceanography: Methods*, 15, 586–600.
1054   doi: 10.1002/lom3.10189

1055 Oueiny, C., Berlioz, S., & Perrin, F.-J. (2014). Carbon nanotube–polyaniline composites. *Progress in*
1056   *Polymer Science*, 39(4), 707–748. doi: 10.1016/j.progpolymsci.2013.08.00

1057 Pan, Y., Sun, Z., He, H., Li, Y., You, L., & Zheng, H. (2018). An improved method of preparing iridium
1058   oxide electrode based on carbonate-melt oxidation mechanism. *Sensors and Actuators B:*
1059   *Chemical*, 261, 316-324. doi: 10.1016/j.snb.2018.01.069

1060 Pandey, P.C., & Singh, G. (2001). Tetraphenylborate doped polyaniline based novel pH sensor and
1061   solid-state urea biosensor. *Talanta*, 55(4), 773–782. doi: 10.1016/S0039-9140(01)00505-7

1062 Parizi, K.B., Yeh, A.J., Poon, A.S.Y., & Wong, H.S.P. (2012). Exceeding Nernst limit (59mV/pH):
1063   CMOS-based pH sensor for autonomous applications. *2012 International Electron Devices*
1064   *Meeting*, 24.7.1 - 24.7.4. doi: 10.1109/IEDM.2012.6479098

1065 Park, H.J., Yoon, J.H., Lee, K.G., & Choi, B.G. (2019). Potentiometric performance of flexible pH
1066   sensor based on polyaniline nanofiber arrays. *Nano Convergence*, 6(1), Article n. 9. doi:
1067   10.1186/s40580-019-0179-0

1068   Park, I., Li, Z., Pisano, A.P., & Williams, R.S. (2010). Top-down fabricated silicon nanowire sensors
1069   for real-time chemical detection. *Nanotechnology*, 1, 015501. doi: 10.1088/0957-4484/21/1/015501

1070   Patil, S., Ghadi, H., Ramgir, N., Adhikari, A., & Rao, V.R. (2019). Monitoring soil pH variation using
1071   Polyaniline/SU-8 composite film based conductometric microsensor. *Sensors and Actuators B:*
1072   *Chemical*, 286, 583-590. doi: 10.1016/j.snb.2019.02.016

1073   Persaud, K.C., & Pelosi, P. (1985). An approach to an artificial nose. *Transactions - American Society*
1074   *for Artificial Internal Organs*, 31, 297–300.

1075   Pfattner, R., Foudeh, A.M., Chen, S., Niu, W., Matthews, J.R., He, M., & Bao, Z. (2019). Dual-Gate
1076   Organic Field-Effect Transistor for pH Sensors with Tunable Sensitivity. *Advanced Electronic*
1077   *Materials*, 5(1), Article n. 1800381. doi: 10.1002/aelm.201800381

1078   Poma, N., Vivaldi, F., Bonini, A., Carbonaro, N., Di Rienzo, F., Melai, B., Kirchhain, A., Salvo, P.,
1079   Tognetti, A., & Di Francesco, F. (2019). Remote monitoring of seawater temperature and pH by
1080   low cost sensors. *Microchemical Journal*, 148, 248-252. doi: 10.1016/j.microc.2019.05.001

1081   Pyo, J.-Y., & Cho, W.-J. (2017). High-performance SEGISFET pH Sensor using the structure of
1082   double-gate a-IGZO TFTs with engineered gate oxides. *Semiconductor Science and Technology*,
1083   32(3), Article N. 035015. doi: 10.1088/1361-6641/aa584b

1084   Qin, Y., Kwon, H.-J., Subrahmanyam, A., Howlader, M.M.R., Selvaganapathy, P.R., Adronov, A., &
1085   Deen, M.J. (2016). Inkjet-printed bifunctional carbon nanotubes for pH sensing. *Materials Letters*,
1086   176, 68–70. doi: 10.1016/j.matlet.2016.04.048

1087   Radu, A., Anastasova, S., Fay, C., Diamond, D., Bobacka, J. & Lewenstam, A. (2010). Low cost,
1088   calibration-free sensors for in situ determination of natural water pollution. *SENSORS, 2010 IEEE,*
1089   1487-1490. doi: 10.1109/ICSENS.2010.5690357

1090   Rahimi, R., Ochoa, M., Parupudi, T., Zhao, X., Yazdi, I.K., Dokmeci, M.R., Tamayol, A.,
1091   Khademhosseini, A., & Ziaie, B. (2016). A low-cost flexible pH sensor array for wound
1092   assessment. *Sensors and Actuators B: Chemical*, 229, 609–617. doi: 10.1016/j.snb.2015.12.082

1093   Ramanathan, T., Abdala, A.A., Stankovich, S., Dikin, D.A., Herrera-Alonso, M., Piner, R.D., Adamson,
1094   D.H., Schniepp, H.C., Chen, X., Ruoff, R.S., Nguyen, S.T., Aksay, I.A., Prud'Homme, R.K., &
1095   Brinson, LC.(2008). Functionalized graphene sheets for polymer nanocomposites. *Nature*
1096   *Nanotechnology*, 3(6), 327-331. doi: 10.1038/nnano.2008.96

1097   Rérolle, V.M.C., Floquet, C.F.A., Mowlem, M.C., Connelly, D.P., Achterberg, E.P., & Bellerby,
1098   R.R.G.J. (2012). Seawater-pH measurements for ocean-acidification observations. *TrAC Trends in*
1099   *Analytical Chemistry,* 40, 146-157. doi: 10.1016/j.trac.2012.07.016

1100   Rérolle, V.M.C., Achterberg, E.P., Ribas-Ribas, M., Kitidis, V., Brown, I., Bakker, D.C.E., Lee, G.A., &
1101   Mowlem, M.C. (2018). High Resolution pH Measurements Using a Lab-on-Chip Sensor in Surface
1102   Waters of Northwest European Shelf Seas. *Sensors*, 18(8), 2622. doi: 10.3390/s18082622

1103   Ribotti, A., Magni, P., Borghini; M., Schroeder, K., Barton, J., McCaul, M., Diamond, D., (2015), New
1104   cost-effective, interoperable sensors tested on existing ocean observing platforms in application of
1105   European directives: The COMMON SENSE European project. *Proceedings of the IEEE OCEANS*
1106   *2015 Conference*, 1-9. doi: 10.1109/OCEANS-Genova.2015.7271340

1107   Saba, G.K., Wright-Fairbanks, E., Chen, B., Cai, W.-J., Barnard, A.H., Jones, C.P., Branham, C.W.,
1108   Wang, K., & Miles, T. (2019). The Development and Validation of a Profiling Glider Deep ISFET-
1109   Based pH Sensor for High Resolution Observations of Coastal and Ocean Acidification. *Frontiers*
1110   *in Marine Science*, 6, Article n. 664. doi: 10.3389/fmars.2019.00664

1111   Sadig, H.R., Cheng, L., & Xiang, T. (2018). Using sol-gel supported by novel economic and
1112   environment-friendly spray-coating in the fabrication of nanostructure tri-system metal oxide-based
1113   pH sensor applications. *Journal of Electroanalytical Chemistry*, 827, 93-102. doi:
1114   10.1016/j.jelechem.2018.09.017

1115   Salaün, A-C., Pichon, L., & Wenga, G. (2014). Polysilicon nanowires FET as highly-sensitive pH-
1116   sensor: modeling and measurements. *Procedia Engineering*, 87, 911 – 914.
1117   doi:10.1016/j.proeng.2014.11.303

1118   Salavagione, H.J., Diez-Pascual, A.M., Lazaro, E., Vera, S., & Gomez-Fatou, M.A. (2014). Chemical
1119   sensors based on polymer composites with carbon nanotubes and graphene: the role of the
1120   polymer. *Journal of Materials Chemistry A*, 2, 14289. doi: 10.1039/C4TA02159B

1121   Salvo, P., Calisi, N., Melai, B., Cortigiani, B., Mannini, M., Caneschi, A., Lorenzetti, G., Paoletti, C.,
1122   Lomonaco, T., Paolicchi, A., Scataglini, I., Dini, V., Romanelli, M., Fuoco, R., & Di Francesco, F.
1123   (2017). Temperature and pH sensors based on graphenic materials. *Biosensors and*
1124   *Bioelectronics*, 91, 870-877. doi: 10.1016/j.bios.2017.01.062

1125   Santos, L., Neto, J.P., Crespo, A., Nunes, D., Costa, N., Fonseca, I.M., Barquinha, P., Pereira, L.,
1126   Silva, J., Martins, R., & Fortunato, E. (2014). WO3 nanoparticle-based conformable pH sensor.
1127   *ACS Applied Materials and Interfaces*, 6(15), 12226-12234. doi: 10.1021/am501724h

1128   Segut, O., Lakard, B., Herlem, G., Rauch, J.-Y., Jeannot, J.-C., Robert, L., & Fahys, B. (2007).
1129   Development of miniaturized pH biosensors based on electrosynthesized polymer films. *Analytica*
1130   *Chimica Acta*, 597(2), 313-321. doi: 10.1016/j.aca.2007.06.053

1131   Sha, R., Komori, K., & Badhulika, S. (2017). Amperometric pH Sensor Based on Graphene-
1132   Polyaniline Composite. *IEEE Sensors Journal*, 17(16), Article n. 7959556, 5038-5043. doi:
1133   10.1109/JSEN.2017.2720634

1134   Sharma, B.K., & Ahn, J.-H. (2013). Graphene based field effect transistors: Efforts made towards
1135   flexible electronics. *Solid-State Electronics*, 89, 177–195. doi:10.1016/j.sse.2013.08.007

1136   Shirale, D.J., Bangar, M.A., Chen, W., Myung, N.V., & Mulchandani, A. (2010). Effect of aspect ratio
1137   (length:diameter) on a single polypyrrole nanowire FET device. *Journal of Physical Chemistry C*,
1138   114, 13375–13380. doi: 10.1021/jp104377e

1139 Singh, K., Lou, B.-S., Her, J.-L., Pang, S.-T., & Pan, T.-M. (2019). Super Nernstian pH response and

1140   enzyme-free detection of glucose using sol-gel derived RuO_x on PET flexible-based extended-gate

1141   field-effect transistor. *Sensors and Actuators B: Chemical*, 298, Article n.126837. doi:

1142   10.1016/j.snb.2019.126837

1143 Sohn, I.-Y., Kim, D.-J., Jung, J.-H., Yoon, O.J., Thanh, T.N., Quang, T.T.,& Lee, N.E. (2013). pH

1144   sensing characteristics and biosensing application of solution-gated reduced graphene oxide field-

1145   effect transistors. *Biosensors and Bioelectronics*, 45, 70–76. doi: 10.1016/j.bios.2013.01.051

1146 Somero, G.N., Beers, J.M., Chan, F., Hill, T.M., Klinger, T., & Litvin, S.Y. (2016). What changes in the

1147   carbonate system, oxygen, and temperature portend for the Northeastern Pacific Ocean: A

1148   physiological perspective. *BioScience*, 66, 14–26. doi: 10.1093/biosci/biv162

1149 Sophocleous, M., & Atkinson, J.K. (2017). A review of screen-printed silver/silver chloride (Ag/AgCl)

1150   reference electrodes potentially suitable for environmental potentiometric sensors. *Sensors and*

1151   *Actuators A: Physical*, 267, 106-120. doi: 10.1016/j.sna.2017.10.013

1152 Sørensen, S.P.L. (1909). Enzymstudien II: Uber die Messung und die Bedeutung der

1153   Wasserstoffionenkonzentration bei enzymatischen Prozessen. *Biochemie Zeitung*, 21, 131-200.

1154   https://d-nb.info/1125891521/34

1155 Spijkman, M., Myny, K., Smits, E.C.P., Heremans, P., Blom, P.W.M., & de Leeuw, D.M. (2011a) Dual-

1156   Gate Thin-Film Transistors, Integrated Circuits and Sensors. *Advanced Materials*, 23(29), 3231-

1157   3242. doi: 10.1002/adma.201101493

1158 Spijkman, M., Smits, E., Cillessen, J.F.M., Biscarini, F., Blom, P.W.M., & de Leeuw, D.M. (2011b).

1159   Beyond the Nernst-limit with dual-gate ZnO ion-sensitive field-effect transistors. *Applied Physics*

1160   *Letters*, 98(4), 043502-043502-3. doi: 10.1063/1.3546169

1161 Staudinger, C., Strobl, M., Breininger, J., Klimant, I., & Borisov, S.M. (2019). Fast and stable optical

1162   pH sensor materials for oceanographic applications. *Sensors and Actuators B: Chemical*, 282,

1163   204-217. doi: 10.1016/j.snb.2018.11.048

1164 Staudinger, C., Strobl, M., Fischer, J.P., Thar, R., Mayr, T., Aigner, D., Müller, B.J., Müller, B., Lehner,

1165   P., Mistlberger, G., Fritzsche, E., Ehgartner, J., Zach, P.W., Clarke, J.S., Geißler, F., Mutzberg, A.,

1166   Müller, J.D., Achterberg, E.P., Borisov, S.M., & Klimant, I. (2018). A versatile optode system for

1167   oxygen, carbon dioxide, and pH measurements in seawater with integrated battery and logger.

1168   *Limnology and Oceanography: Methods*, 16(7), 459–473. doi: 10.1002/lom3.10260

1169 Stow, C.A., Jolliff, J., McGillicuddy Jr., D.J., Doney, S.C., Allen, J.I., Friedrichs, M.A.M., Rose, K.A., &

1170   Wallhead, P. (2009). Skill assessment for coupled biological/physical models of marine systems.

1171   *Journal of Marine Systems*, 76(1-2), 4–15. doi: 10.1016/j.jmarsys.2008.03.011

1172 Su, W., Xu, J., & Ding, X. (2016). An Electrochemical pH Sensor Based on the Amino-Functionalized

1173   Graphene and Polyaniline Composite Film. *IEEE Transactions on Nanobioscience*, 15, 8. doi:

1174   10.1109/TNB.2016.2625842

1175 Sulka, G.D., Hnida, K., & Brzózka, A. (2013). pH sensors based on polypyrrole nanowire arrays.
1176 *Electrochimica Acta*, 104, 536– 541. doi: 10.1016/j.electacta.2012.12.064

1177 Takechi, K., Iwamatsu, S., Konno, S., Yahagi, T., Abe, Y., Katoh, M., & Tanabe, H. (2015). Gate-to-
1178 source voltage response in high-sensitivity amorphous InGaZnO$_4$ thin-film transistor pH sensors.
1179 *Japanese Journal of Applied Physics*, 54(7), 078004. doi: 10.7567/jjap.54.078004

1180 Tan, X., Chuang, H.-J., Lin, M.-W., Zhou, Z., & Cheng, M. M.-C. (2013). Edge Effects on the pH
1181 Response of Graphene Nanoribbon Field Effect Transistors. *Journal of Physical Chemistry C*,
1182 117(51), 27155–27160. doi: 10.1021/jp409116r

1183 Tasis, D., Tagmatarchis, N., Bianco, A., & Prato, M. (2006). Chemistry of carbon nanotubes. *Chemical*
1184 *Reviews*, 106(3), 1105-1136. doi: 10.1021/cr050569o

1185 Trasatti, S. (1991). Physical electrochemistry of ceramic oxides. *Electrochimica Acta*, 36, 225–241.
1186 doi: 10.1016/0013-4686(91)85244-2

1187 Tsai, Y.-T., Chang, S.-J., Ji, L.-W., Hsiao, Y.-J., & Tang, I.-T. (2019). Fast Detection and Flexible
1188 Microfluidic pH Sensors Based on Al-Doped ZnO Nanosheets with a Novel Morphology. *ACS*
1189 *Omega*, 4(22), 19847-19855. doi: 10.1021/acsomega.9b02778

1190 Uria, N., Abramova, N., Bratov, A., Muñoz-Pascual, F.-X., & Baldrich, E. (2016). Miniaturized metal
1191 oxide pH sensors for bacteria detection. *Talanta*, 147, 364–369. doi: 10.1016/j.talanta.2015.10.011

1192 Weldborg, M., Turner, D.R., Anderson, L.G., & Dyrssen, D. (2009). Determination of pH. In K.
1193 Grasshoff, K. Kremling, & M.Ehrhardt (Eds.), *Methods of Seawater Analysis*, John Wiley & Sons.

1194 Wu, Y.-C., Wu, S.-J., & Lin, C.-H. (2017). Mass-produced polyethylene-terephthalate film coated with
1195 tantalum pentoxide for pH measurement under ISFET detection configuration. *Microsystem*
1196 *Technologies*, 23(2), 293-298. doi: 10.1007/s00542-015-2474-y

1197 Xu, K., Zhang, X., Hou, K., Geng, M., & Zhao, L. (2016). The effects of antimony thin film thickness on
1198 antimony pH electrode coated with nafion membrane. *Journal of the Electrochemical Society*,
1199 163(8), B417-B421. doi: 10.1149/2.0191608jes

1200 Xu, K., Zhang, X., Chen, C., & Geng, M. (2018). Development and Performance of an All-Solid-Stated
1201 pH Sensor Based on Modified Membranes. *International Journal of Electrochemical Science,* 13,
1202 3080-3090. doi: 10.20964/2018.03.04

1203 Yao, S., Wang, M., & Madou, M. (2001). A pH Electrode Based on Melt-Oxidized Iridium Oxide.
1204 *Journal of the Electrochemical Society*, 148(4), H29-H36. doi: 10.1149/1.1353582

1205 Yoon, J.H., Hong, S.B., Yun, S.-O., Lee, S.J., Lee, T.J., Lee, K.G., Choi, B.G. (2017). High
1206 performance flexible pH sensor based on polyaniline nanopillar array electrode. *Journal of Colloid*
1207 *and Interface Science*, 490, 53–58. doi: 10.1016/j.jcis.2016.11.033

1208 Young, S.-J., & Tang, W.-L. (2019). Wireless Zinc Oxide Based pH Sensor System. *Journal of the*
1209 *Electrochemical Society*, 166(9), B3047-B3050. doi: 10.1149/2.0071909jes

1210   Zea, M., Moya, A., Fritsch, M., Ramon, E., Villa, R., & Gabriel, G. (2019). Enhanced Performance
1211   Stability of Iridium Oxide-Based pH Sensors Fabricated on Rough Inkjet-Printed Platinum. *ACS*
1212   *Applied Materials and Interfaces*, 11(16), 15160-15169. doi: 10.1021/acsami.9b03085

1213   Zhang, X., Ye, Y., Kan, Y., Huang, Y., Jia, J., Zhao, Y.Chen, C.-T.A., Qin, H. (2017). A new
1214   electroplated Ir/Ir(OH)$_x$ pH electrode and its application in the coastal areas of Newport Harbor,
1215   California. *Acta Oceanologica Sinica*, 36 (5), 99–104. doi: 10.1007/s13131-017-1064-5

1216   Zhang, W.-D., & Xu, B. (2009). A solid-state pH sensor based on WO$_3$-modified vertically aligned
1217   multiwalled carbon nanotubes. *Electrochemistry Communications*, 11, 1038–1041.
1218   doi:10.1016/j.elecom.2009.03.006

1219   Zhao, R., Xu, M., Wang, J., & Chen, G. (2010). A pH sensor based on the TiO$_2$ nanotube array
1220   modified Ti electrode. *Electrochimica Acta*, 55 (20), 5647-5651.
1221   doi:10.1016/j.electacta.2010.04.102

1222   Zhao, W.-S., Fu, K., Wang, D.-W., Li, M., Wang, G., Yin, W.-Y. (2019). Mini-review: modeling and
1223   performance analysis of nanocarbon interconnects. *Applied Sciences*, 9 (11), 2174.
1224   doi:10.3390/app9112174

1225   Zhu, Y., Wang, C., Petrone, N., Yu, J., Nuckolls, C., Hone, J., & Lin, Q. (2015). A solid-gated
1226   graphene FET sensor for pH measurements. In *Proceedings of the IEEE International Conference*
1227   *on Micro Electro Mechanical Systems (MEMS)*. doi: 10.1109/MEMSYS.2015.7051097

1228   Zuaznabar-Gardona, J.C., & Fragoso, A. (2018). A wide-range solid state potentiometric pH sensor
1229   based on poly-dopamine coated carbon nano-onion electrodes. *Sensors and Actuators B:*
1230   *Chemical*, 273, 664-671. doi: 10.1016/j.snb.2018.06.103